

Division of Engineering
BROWN UNIVERSITY
PROVIDENCE, R. I.

RADIATIVE TRANSFER IN A GAS
OF UNIFORM PROPERTIES IN LOCAL
THERMODYNAMIC EQUILIBRIUM
PART 2: RELATIVE LINE INTENSITIES
AND THE TREATMENT OF WEAK LINES

B. L. HUNT and M. SIBULKIN

DDC
R
MAR 17 1967
REF ID: A65001760
B

Best Available Copy

Advanced Research Projects Agency
Ballistic Missile Defense Office
and the Fluid Dynamics Branch
Office of Naval Research

Report No.

Nonr-562 (35)/17

ARCHIVE COPY

December 1966

RADIATIVE TRANSFER IN A GAS OF UNIFORM PROPERTIES
IN LOCAL THERMODYNAMIC EQUILIBRIUM
PART 2: RELATIVE LINE INTENSITIES AND
THE TREATMENT OF WEAK LINES

by

Brian L. Hunt and Merwin Sibulkin

Division of Engineering
Brown University
Providence, Rhode Island

December 1966

This work was supported by the Advanced Research Projects Agency (Ballistic Missile Defense Office) and by the Fluid Dynamics Branch of the Office of Naval Research under contract Nonr 562(35), Task NR 061-132.

Reproduction in whole or in part is permitted for any purpose of the United States Government. Distribution of this document is unlimited.

SUMMARY

This report is concerned with the transfer of radiative energy by the lines of a gas of uniform properties in local thermodynamic equilibrium.

By means of comparatively simple calculations, the relative intensities of the potentially strong lines of a simple (hydrogenic) spectrum are computed and these results are interpreted in detail. An important conclusion from these calculations is that the influences of lower state occupation number and line oscillator strength can, under some conditions, be outweighed by factors such as the line width and the local value of the Planck function.

The remainder of the report is concerned with the numerous weak lines associated with high quantum numbers. It is shown that these lines can be allowed for by extending the cross sections of the appropriate continuum processes. These techniques are then used to compare the intensities of groups of weak lines with the intensities of certain strong lines.

TABLE OF CONTENTS

SUMMARY

PRINCIPAL SYMBOLS

1. INTRODUCTION
2. RELATIVE INTENSITIES OF ELECTRON IMPACT BROADENED LINES
 - 2.1 Introduction
 - 2.2 Self-Absorbed Leading Lines
 - 2.3 Self-Absorbed Lines within the Same Series
 - 2.4 Optically Thin Leading Lines
 - 2.5 Optically Thin Lines within the Same Series
3. THE TREATMENT AND IMPORTANCE OF WEAK LINES
 - 3.1 Introduction
 - 3.2 Line Merging and the Apparent Depression of the Ionization Limit
 - 3.3 Treatment of High Lines
 - 3.4 Importance of High Lines
 - 3.5 Treatment of Lines and Photoionization from Highly Excited Lower States
 - 3.6 Importance of Lines and Photoionization from Highly Excited States

APPENDIX I. Optically Thin Radiation from High Lines and the Bound-Free Continuum

APPENDIX II. The Use of the Bound-Free Continuum Absorption Coefficient to Represent Self-Absorbed, Effectively Merged High Lines

APPENDIX III. Self-Absorption of the Extended Continuum Corresponding to Optically Thin Lines

References

Figures

PRINCIPAL SYMBOLS

Σ_v	Planck function
c	velocity of light in a vacuum
e	charge of electron
E_m	energy of electronic state with principal quantum number m
f_{mn}	absorption oscillator strength for a transition from a state with principal quantum number m to a state with principal quantum number n
$F(m, t)$	function defined by Eq. (3.5)
g_m	statistical weight of the state with principal quantum number m
h	Planck's constant
I_v	specific intensity of radiation
I	frequency integrated specific intensity of radiation, $\int_0^{\infty} I_v dv$
I_{mn}	I for the isolated line with quantum numbers m and n .
k	Boltzmann's constant
K_v	linear spectral absorption coefficient
m	principal quantum number of lower state
\bar{m}	lower state quantum number corresponding to the first high series which is completely merged according to effective widths or is completely optically thin
m^*	the sum of the intensities of either all lines or all transitions with $m \geq m^*$ is equal to 10% of the intensity of the leading line
m_e	mass of electron
n	principal quantum number of upper state

\bar{n}	upper state quantum number of the first high line which is either merged according to its effective width or optically thin
n^*	the sum of the intensities of all lines with $n \geq n^*$ is equal to 10% of the intensity of the series leading line
N_a	number density of atoms
N_e	number density of electrons
N_L	Loschmidt number ($2.6871 \times 10^{19} \text{ cm}^{-3}$)
N_m	number density of particles with principal quantum number m
N_z	number density of particles with charge z
p	$n - m$
Ω_a	electronic partition function of an atom
Ω_i	electronic partition function of an ion
Ry	Rydberg energy constant
s	path length
\bar{s}	$s N_e / N_L$
τ	χ_H / kT
T	temperature
w	line width parameter
W	effective width of intensity profile
z	number of charges
z_r	charge on radiating particle
z_p	charge on perturbing particle
Δv_C	interline spacing
v	frequency
v_{mn}	center frequency for a transition from a state with principal quantum number m to a state with principal quantum number n .

τ optical depth of a line, $(\int_0^{\infty} K_v dv/w)s$

χ ionization potential

χ_H ionization potential of hydrogen

1. INTRODUCTION

It is well known that when a space vehicle enters a planetary atmosphere radiative mechanisms are important in the transfer of energy from the locally heated gas to the vehicle; one of the current interests in this problem is in the role of spectral lines in the transfer process.¹ However, the task of computing the line intensities in even an isothermal slab of gas is extremely involved due to the complexity of the line spectra. If one is to attempt such computations and interpret the results meaningfully, it is necessary to make approximations which reduce the immense number of transitions to a more tractable number. The problem of making such approximations is made considerably easier by an understanding of the interaction of the various factors which contribute to the radiative intensity of a line. This understanding can be gained in part from previous work. Some relevant papers are due to Allen,² Biberman and coworkers,^{3,4} Olfe⁵ and Aroeste and Benton.⁶ The purpose of this Part is to supplement the results already available with a more detailed investigation of relative line intensities.

Throughout this Part the line positions and oscillator strengths used are those of hydrogen. These values have the advantage of being obtainable from simple analytic expressions and although the resulting spectrum is simpler than that of a nonhydrogenic gas, it displays most of the main features. In contrast, the line profiles of hydrogen are not typical of other gases (and are generally more complex). Therefore, since the main concern in this work is with nonhydrogenic gases, we choose the line profiles to be representative of a nonhydrogenic gas.

Chapter 2 describes some comparatively simple calculations on the relative intensities of the stronger lines and gives a detailed physical interpretation. Chapter 3 is concerned with the treatment of weak lines. New methods of treating these lines are described and then used to indicate the importance of such lines relative to stronger lines.

2. RELATIVE INTENSITIES OF ELECTRON IMPACT BROADENED LINES2.1 Introduction

The strongest lines of a nonhydrogenic gas correspond to transitions between states of relatively low excitation. Such lines are predominantly broadened by electron impacts (see Part 1, Chap. 4) which give rise to dispersion profiles. The growth of intensity of a dispersion line has been described in Part 1, Section 3.3 where it was shown that two simple asymptotic expressions describe the growth to a good approximation. The expression for small optical depth is

$$I = B_{v_0} s \int_0^{\infty} K_v dv \quad (2.1)$$

and the expression for large optical depth is

$$I = 2B_{v_0} (ws \int_0^{\infty} K_v dv)^{1/2}. \quad (2.2)$$

These curves intersect at the point

$$s \int_0^{\infty} K_v dv / w = 4 \quad (2.3)$$

In order to evaluate Eq. (2.1) or Eq. (2.2) one needs to know the end states of the transition, the thermodynamic state (n, T) and the path length, s .

For a line between lower state m and upper state n we have for the absorption coefficient

$$\int_0^{\infty} K_{v_{mn}} dv = \frac{\pi^2}{m_e c} N_m f_{mn} [1 - \exp(-\frac{hv_{mn}}{kT})] \quad (2.4)$$

where N_m is the number density of particles in the lower state m , f_{mn} is the oscillator strength (see Section 3.2 of Part 1) and the factor $1 - \exp(-hv/kT)$ makes allowance for stimulated emission. The occupation number N_m^{mn} is related to the total number of particles, N , by the Boltzmann formula (Part 1, Section 2.1),

$$N_m^{mn} = \rho_m \exp(-E_m) N / \Omega_{el} \quad (2.5)$$

where E_m and ρ_m are the energy and statistical weight respectively for the lower state m and Ω_{el} is the electronic partition function.

For hydrogen, the frequencies, energy levels and oscillator strengths are given by the following expressions⁷

$$hv_{mn} = E_n - E_m = x_H \left(\frac{1}{m^2} - \frac{1}{n^2} \right) \quad (2.6)$$

and

$$f_{mn} = \frac{2^6}{3\sqrt{3}\pi} \frac{1}{\rho_m} \frac{1}{n^3 m^3} \frac{1}{(1/m^2 - 1/n^2)^3} \quad (2.7)$$

where x_H is the Rydberg energy. Finally, we need an expression for the line width w . A detailed discussion of nonhydrogenic line widths has been given in Part 1, Section 4.5. In that discussion, two approximate expressions for electron impact line widths in a hydrogenic spectrum were given. The first expression, based on adiabatic theory and due to Margenau and Lewis,⁸ is

$$w \text{ eV} = 0.98 \times 10^{-23} \left(\frac{n_u}{z} \right)^4 (N_e \text{ cm}^{-3}) (kT \text{ eV})^{1/6} \quad (2.8)$$

where n_u is the principal quantum number of the upper state and N_e is the number density of electrons. The other expression, valid for inelastic collisions and first given by Stewart and Pyatt,⁹ is

$$w \text{ eV} = 3.3 \times 10^{-22} \frac{n_u^4}{z^2} (N_e \cdot \text{cm}^{-3}) (kT \text{ eV})^{-1/2}. \quad (2.9)$$

For our present purposes it is interesting that despite their other differences, the two expressions Eqs. (2.8) and (2.9) are each of the form

$$w = N_e f(T, z) n_u^4. \quad (2.10)$$

In this chapter it will not be necessary to specify $f(T, z)$ since we will restrict ourselves to comparing pairs of lines which are such that either both are self-absorbed or neither is self-absorbed.

The ratio of intensities of two lines which are both self-absorbed can be obtained from Eqs. (2.2), (2.4) and (2.5) in the form

$$\frac{I_{mn}}{I_{m'n'}} = \frac{B_{v_{mn}}}{B_{v_{m'n'}}} \frac{\frac{w_{mn} g_m f_{mn} [1 - \exp(-hv_{mn}/kT)]}{w_{m'n'} g_{m'} f_{m'n'} [1 - \exp(-hv_{m'n'}/kT)]}}{\exp(-\frac{E_m - E_{m'}}{2kT})}^{1/2}. \quad (2.11)$$

Then, if the explicit form of the Planck function

$$B_{v_{mn}} = \frac{2h}{c^2} \frac{v^3}{\exp(hv_{mn}/kT) - 1}, \quad (2.12)$$

the hydrogenic expressions Eqs. (2.6) and (2.7) and the general line width formula Eq. (2.10) are inserted into Eq. (2.11) the following result is obtained

$$\frac{I_{mn}}{I_{m'n'}} = \left\{ \frac{n}{n'} \left(\frac{m'}{m} \right)^3 \left(\frac{1/m^2 - 1/n^2}{1/m'^2 - 1/n'^2} \right)^3 \frac{\exp(t/n^2)}{\exp(t/n'^2)} \frac{\exp[t(1/m'^2 - 1/n'^2)] - 1}{\exp[t(1/m^2 - 1/n^2)] - 1} \right\}^{1/2}. \quad (2.13)$$

where $t \equiv x_H/kT$.

In contrast to the case for absolute intensities, Eq. (2.13) is independent of ρ and s . Sections 2.2 and 2.3 apply Eq. (2.13) to the

leading lines of different series and different lines of the same series respectively.

In the case of two lines which are not self-absorbed, Eq. (2.1) holds. Substituting in this equation the hydrogenic energy and oscillator strength expressions, one obtains a result analogous to Eq. (2.13), explicitly

$$\frac{I_{mn}}{I_{m'n'}} = \left(\frac{n'm'}{mn} \right)^3 \frac{\exp(t/n^2)}{\exp(t/n'^2)}. \quad (2.14)$$

Sections 2.4 and 2.5 apply Eq. (2.14) to the classes of lines treated in Sections 2.2 and 2.3.

Some caution is required in applying results obtained in this chapter to lines with moderately high quantum number upper states. Such lines can have different profiles from those with low quantum number upper states. (See Part 1, Section 4.6, for a discussion of this effect in nitrogen.) The line width expression (Eq. 2.10) used in the calculations presented here may therefore break down for some higher quantum number transitions.

Finally, it must be pointed out that when self-absorption occurs, the background continuum is a factor which is active in determining the relative importance of the lines. This is because lines which occur where the continuum absorption coefficient is large are reduced in importance (see Part 1, Eq. (3.2)). The detailed calculation of Part 3 considers this effect but it is not accounted for in the calculations of this part.

2.2 Self-Absorbed Leading Lines

In this section we compare the intensity of the leading line of a series with an excited lower state to the intensity of the leading line in the series originating from the ground state. Both lines are assumed to be

self-absorbed. The reference line just introduced is sometimes called the resonance line or (since the spectrum is that of hydrogen) the Lyman α line.

The relevant form of Eq. (2.13) is

$$\frac{I_{m,m+1}}{I_{1,2}} = \left(\frac{1}{2} \left(\frac{4}{3} \right)^3 \frac{\exp[t/(m+1)^2]}{\exp(t/4)} \frac{(2m+1)^3}{m^9(m+1)^5} \frac{\exp(3t/4) - 1}{\exp[(2m+1)t/m^2(m+1)^2] - 1} \right)^{1/2}. \quad (2.15)$$

The quantity $I_{m,m+1}/I_{1,2}$ is shown on Fig. 1 for several values of m and a wide range of t . The asymptotic limit of $t \rightarrow 0$ is also shown for comparison. The analytic expression for this limit is easily obtained from Eq. (2.15) and is

$$\lim_{t \rightarrow 0} \frac{I_{m,m+1}}{I_{1,2}} = \frac{4}{3} \left[\frac{1}{2} \frac{(2m+1)^2}{m^7(m+1)^3} \right]^{1/2} \quad (2.16)$$

The factors which combine to produce the results displayed on Fig. 1, and their independent effects, are as follows. Line broadening increases with upper state quantum number and hence tends to increase the intensities of the higher series lines. Values of g_f slightly favor the higher series lines. The unweighted occupation numbers, $\exp(-E_m/kT)/Q_{ei}$, favor the resonance line. The factor due to stimulated emission decreases with frequency and hence acts against the low frequency high series lines. Finally, there is the value of the Planck function. This factor can emphasize either the high series line or the resonance line depending on the position of the line centers with respect to the position of the Planck maximum.

Figure 2 is intended as an aid to discussion of the influence of the Planck function. It shows the Planck function plotted against the similarity parameter hv/kT . In terms of this variable, the positions of the line centers (which are at constant frequency) change with temperature. This movement of line centers is linear with t and is shown for a number of

lines on Fig. 2. At very high temperatures $t \rightarrow 0$ and all the lines are to the left of the Planck maximum with the 1st Lyman line (Lyman α) nearest to the maximum. The Planck function will therefore favor radiation from the Lyman line. As the temperature falls, the lines move towards the Planck maximum until at $t = 3.8$ the 1st Lyman line reaches the maximum and, thereafter, the associated value of the Planck function will start to fall while those of the other leading lines continue to rise until they too in turn pass over the maximum.

As shown by Fig. 1, this influence of the Planck function is the dominant effect. In particular it can be seen that at low temperatures (i.e. high values of t) the intensities of the higher series lines can become greater than that of the Lyman line. At these high values of t , the influence of B_ν is in opposition to those of induced emission (which is small anyway) and the Boltzmann distribution but whereas the intensity is linear in B_ν , it varies as the square root of the Boltzmann distribution factor and also as the square root of the stimulated emission factor (see, Eq. 2.11). At low values of t , these three effects reinforce each other to produce dominance of the Lyman α line.

2.3 Self-Absorbed Lines Within the Same Series

In this section we compare lines within the same series (i.e. having the same value of m). The reference line is chosen to be the series leading line.

The appropriate form of Eq. (2.13) is

$$\frac{I_{m,m+p}}{I_{m,m-1}} = \left(\left(\frac{2mp+p^2}{2m+1} \right)^3 \left(\frac{m+1}{m+p} \right)^5 \frac{\exp[t/(m+p)^2]}{\exp[t/(m+1)^2]} \frac{\exp[(2m+1)t/m^2(m+1)^2]-1}{\exp[(2mp+p^2)t/m^2(m+p)^2]-1} \right)^{1/2} \quad (2.14)$$

where $m+p = n$. The asymptotic limit for small t is

$$\lim_{t \rightarrow 0} \frac{I_{m,m+p}}{I_{m,m+1}} = \frac{2mp + p^2}{2m + 1} \left(\frac{m+1}{m+p} \right)^{3/2}. \quad (2.18)$$

A further asymptotic limit which is outside the range of validity of our assumptions but exhibits an interesting trend is that of $m \rightarrow \infty$. The formal limit is

$$\lim_{m \rightarrow \infty} \frac{I_{m,m+p}}{I_{m,m+1}} = p \quad (2.19)$$

Equations (2.17), (2.18) and (2.19) have been evaluated and are plotted on Figs. 3a, 3b and 3c for $m = 1, 2$ and 3 respectively.

The relative intensities of lines within the same series are not affected by population densities since each line starts from the same lower state. Line broadening favors the upper lines while the oscillator strength is greatest for the leading line. Of these two factors, the line width is the stronger effect at high values of n since then $1/m^2 - 1/n^2$ is approximately constant with n so that $f_{mn} \propto n^{-3}$ while $w \propto n^4$. It is this effect which is responsible for the upward trend at high values of p shown on Fig. 3. Since $v_{m,n+1} > v_{m,n}$, stimulated emission decreases with n and thus the intensity tends to rise. The main influence of temperature, however, occurs through the Planck function. Figure 2 shows that

$B_{v_{m,n}} > B_{v_{m,n+1}}$ for the Balmer and higher series except at very low temperatures and for the Lyman series at comparatively high temperatures ($t \gtrsim 3$). These effects are clearly shown on Fig. 3. Further, as m increases the influence of temperature becomes less (because the difference in frequencies becomes less) until, in the limit of very high m , the relative intensities

become independent of temperature (cf. Eq. (2.19)). This trend can be seen by comparing Figs. 3a, 3b and 3c.

2.4 Optically Thin Leading Lines

When the Lyman α line is optically thin, local thermodynamic equilibrium will not normally hold but it is useful for comparison with the results of Section 2.2 to choose the Lyman α as the reference line for this section.

For the present case, Eq. (2.14) becomes

$$\frac{I_{m,m+1}}{I_{1,2}} = \frac{8}{m^3(m+1)^3} \frac{\exp[t/(m+1)^2]}{\exp(t/4)} . \quad (2.20)$$

Values of $I_{m,m+1}/I_{1,2}$ have been obtained from Eq. (2.20) and are plotted on Fig. 4. They are shown both on a linear scale (which is stretched by a factor of 10 compared to Fig. 1) and on a logarithmic scale.

The dominance of the resonance line when it is optically thin is clearly shown by Fig. 4. In terms of the discussion of Section 2.2, we can say that line broadening is no longer a factor and the influence of the Planck function is exceeded by those of the Boltzmann distribution and stimulated emission. Unlike the self-absorbed case, the importance of the high series lines increases with temperature since now the Boltzmann distribution is the determining factor.

Expressing the absolute intensity in terms of the population of the upper state further emphasizes the importance of the resonance line. The following form can easily be obtained from Eqs. (2.1), (2.4) and (2.5)

$$I_{mn} = 2h/c^2 \frac{\pi e^2}{mc} \rho_{n,m}^f v_{mn}^3 \exp(-\Gamma_n/kT) N/N_{el} . \quad (2.21)$$

in which $\rho_{n,m}^f v_{mn}^3 \propto \frac{1}{n^3 m^3}$ so that it can be seen that the resonance line

must always exceed any other leading line. Notice that Eq. (2.21) does not contain B_v because, when the gas is optically thin, only spontaneous emission contributes to the intensity.

2.5 Optically Thin Lines Within the Same Series

This section compares the intensity from the general line $I_{m,m+p}$ to the series leading line $I_{m,m+1}$ when both are optically thin.

Equation (2.14) for this case is

$$\frac{I_{m,m+p}}{I_{m,m+1}} = \left(\frac{m+1}{m+p}\right)^3 \frac{\exp[t/(m+p)^2]}{\exp[t/(m+1)^2]} . \quad (2.22)$$

Values calculated from Eq. (2.22) are presented on Fig. 5. Unlike the case where self-absorption occurs, the ratio $I_{m,m+p}/I_{m,m+1}$ is always less than unity since now line broadening has no influence and the f-number effect is stronger (linear instead of square root). Equation (2.21) is again instructive since $g_n f_{nm} v^3 \propto \frac{1}{n^3 m^3}$ and decreases with n as does $\exp(-E_n/kT)$. Because E_n changes most rapidly for $m = 1$, the Lyman series shows the most rapid fall off. Finally, the change in all series is most rapid for high t because of the factor $\exp(-E_n/kT)$.

3. THE TREATMENT AND IMPORTANCE OF WEAK LINES

3.1 Introduction

Radiation from lines can be calculated by well established methods (see Part 1, Section 3.3) provided the lines do not interfere with each other. A method of accounting for the interference of small groups of lines (such as multiplets) has been described in Part 1, Section 3.4. This chapter is concerned with the problem of the large number of weak, closely spaced lines which are found in any spectrum. These lines can be considered in two classes.

(1) Lines which occur at the high frequency end of series with low quantum number initial states (called here high lines). (2) The complete series which have highly excited initial states (called here high series).

The merging of high lines in an optically thin medium gives rise to an apparent depression of the ionization limit, as is well known (see Section 3.2). The treatment of high lines developed here is related to this apparent depression. An analogous method is also demonstrated for the high series.

The presentation is as follows. Section 3.2 describes briefly the theoretical treatment of the apparent depression of the ionization limit in an optically thin gas. Section 3.3 then presents a method for calculating the radiation from high lines. As an example, the method is applied to a hydrogenic gas in Section 3.4 where, for each of the first three series, the importance of the high lines with respect to the series leading line is calculated. Section 3.5 then presents an analogous method for dealing with high series (and high bound-free transitions). Finally, the application of the method to a hydrogenic gas is demonstrated and the importance of high series with respect to the Lyman α line is examined in Section 3.6.

3.2 Line Merging and the Apparent Depression of the Ionization Limit

As one passes along a series of lines away from the leading line, the inter-line spacing rapidly decreases and at the same time, if the gas is at least partially ionized, the influence of charged particles on the energy levels increases and produces a larger line width. The high lines of a series thus tend to merge and produce the appearance of an extension of the continuum in the direction of lower frequencies. In other words, there is an apparent drop in the ionization potential. The similar behavior of merged, high quantum number states and free states is a consequence of the correspondence principle. The appearance of the absorption coefficient in the merging region is exhibited in papers by Pannekoek¹⁰ and Vidal.¹¹

As we have already seen (Part 1, Chap. 2), there is also a real drop in ionization potential due to the presence of charged particles but it can easily be shown that this drop is less than the apparent drop due to line merging within our range of conditions. Therefore, although it is important for other reasons, such as calculating species composition (see Part 1, Chap. 2), the real depression of ionization limit may be ignored in the study of absorption cross sections and the photo-electric threshold fixed instead from the pseudo-depression due to line merging.

The exact position of the depressed threshold is clearly somewhat arbitrary: Inglis and Teller¹² required that at the threshold the line width at half its peak value be equal to the spacing between line centers and this criterion seems to have been generally adopted. The original paper by Inglis and Teller takes the half-width given by quasi-static theory (see Part 1, Chap. 4, for a discussion of line broadening) whereas recent work by Armstrong¹³ uses the half-width due to inelastic impact broadening by electrons. The resulting expressions are very little different at temperatures of interest to us.

Theoretical results of the type discussed in the previous paragraph locate the position of the apparent photoelectric edge of the absorption coefficient, i.e. the edge which would be observed from an optically thin slab. However, we are not concerned with predicting the spectral appearance of radiation from a thin slab but with the frequency integrated intensity from a slab of variable thickness. In the next section it is shown that the contribution of high lines to the frequency integrated intensity can be obtained by depressing the photoelectric edge even further, specifically, to the first line which is optically thin or to the first line whose effective width (see Part 1, Section 3.3) exceeds the interline spacing, whichever occurs first.

3.3 Treatment of High Lines

Since there is no sharp cut-off point between merged and isolated lines, the lines below the apparent threshold will be overlapping but distinguishable if an optically thin sample is observed. However, when self-absorption occurs, each line is blackened out across the effective width (see Part 1, Section 3.3) which can be considerably greater than the half-width of the absorption coefficient and which is representative of the width of the intensity profile. As a result, merging of the lines observed from an optically thick slab will be more extensive than the merging of the lines emitted by an optically thin slab at the same conditions.

Figure 6 is a sketch contrasting the appearance of the intensity profile with that of the absorption coefficient for a series of lines in which a self-absorbed, isolated line is followed by several effectively merged lines.

One way of treating these merged lines is by computing the black body output over the merged interval (as was done by Biberman et al.¹⁵). It is true that once two successive lines in a series merge all subsequent, higher lines will be merged so long as they are self-absorbed (since the effective width

I/R_{v_0} grows as $n^{1/2}$ for impact broadening or remains constant for quasi-static broadening, whereas the interline spacing falls as n^{-3}). Nonetheless, this approach involves certain complications. In the first place, the lines may become optically thin before the true continuum commences and the thin lines must be treated by another method. Secondly, the background continuum can make no contribution to the total intensity from the gas over the blackened-out interval and an appropriate subtraction must be made from the frequency integrated continuum intensity. Finally, a quite different analysis must be used when the lines are optically thin; integrated expressions for this condition exist (see Ref. 13 and Appendix I) but they do not allow for the variation of the background continuum across the group of lines.

We will now describe an alternative approach which avoids these difficulties. Our method is to extend the bound-free continuum still further down the series, the threshold being fixed by the first pair of lines which are merged according to their effective widths or by the first optically thin line, whichever comes first. The remainder of this section is spent in discussing this method.

In the first place, let us consider an optically thin sample of gas. It is shown in Appendix I that the frequency-integrated intensity from a group of high lines ($n \gg 1$) is equal to the frequency-integrated intensity due to the (extended) bound-free continuum over the same frequency interval. Now, if we start at the first high ($n \gg 1$) line of a series and examine each in turn, then, if we encounter an optically thin line, we know that all higher lines must also be optically thin because the f-numbers decrease along the series (Eq. (2.7)) and the line widths increase. The question remains as to whether the bound-free continuum is also optically thin (since only then does the equivalence demonstrated in Appendix I hold). In this connection, one must observe that whereas the lines are (arbitrarily) considered either thick

or thin, no such sharp division is made for the continuum. Appendix III discusses the problem and concludes that wherever high lines are optically thin, the use of an extended bound-free absorption coefficient will yield a good approximation to the frequency-integrated radiation from the thin high lines. We may therefore extend the bound-free absorption coefficient backwards to the first high, thin line.

Our second problem is to deal with the high lines if they are optically thick. It has been pointed out earlier that self-absorption of high lines will cause extensive merging with the result that the interval over which the lines are merged emits black-body radiation. Now, when the emitted radiation is black-body, any absorption coefficient which is sufficiently large to produce approximately complete self-absorption may be substituted for the actual coefficient. It is shown in Appendix II that the extended bound-free absorption coefficient is sufficiently large in this sense wherever the lines are merged according to their effective widths. Suppose now, that we examine in turn each high line of a series in a self-absorbing medium, starting with the first high line. Then, if we find a self-absorbed line whose effective width exceeds the interline spacing, one of two possibilities can occur with regard to the lines higher up the series. Either they are all self-absorbed or, at some point, a line becomes optically thin. In the first of these two cases, as we have pointed out earlier in this section, all the higher lines are merged and hence their (black-body) intensity can be achieved by using the extended bound-free absorption coefficient. In the second case, from the thin line onwards all the lines must be thin and we have the situation discussed in the preceding paragraph.

According to the arguments just presented, we have two alternative criteria for fixing the position of the pseudo-photoionization threshold: The first criterion is the center frequency of the first high line which is

optically thin, e.g. satisfies $\tau \leq 2^{a/(a-1)}$ where $\tau \equiv (\int_0^\infty K_v dv / w)_s$ and a is the exponent of the wing profile (see Part 1, Section 3.3). The second criterion is the center frequency of the first line whose effective width, w , exceeds the interline spacing, Δv_c . Figure 7 illustrates schematically the two criteria in two cases where they almost coincide. It illustrates the behavior of τ and $w/\Delta v_c$ as one passes along a series of lines. In many cases, in contrast to Fig. 7, either all the high lines will be optically thin or they will all be merged and the start of the pseudo-continuum will occur at the first high line.

According to the analyses of Appendices I and II, the method just described is valid only where the upper state quantum number n is such that $n \gg 1$; we have been referring to lines with upper states satisfying this condition as high. However, it will now be argued that some of the lower lines can also be treated by the pseudo-continuum method. First, suppose the lines are optically thin. Section 2.5 shows that in these circumstances, the intensity carried by each line falls off rapidly along the series. Thus it is only necessary to have an accurate treatment of the first few lines, all the remainder can be included in the pseudo-continuum. Secondly, suppose the lines are self-absorbed and merged. In this case, the interval of black-body radiation extends into the low lines and the extended bound-free absorption coefficient can again be used to produce the radiation in this interval. However, an adaption of the analysis in Appendix II to lower lines shows that when the lines are only just self-absorbed and merged, the continuum absorption coefficient may be too small to produce black-body radiation. Fortunately, the error in the overall intensity produced by this infrequent occurrence will be small. Thus it turns out that, in any series, the only lines which may not be included in the pseudo-continuum

are a few early lines plus any other lines which are both isolated and self-absorbed.

Figure 8 shows for the first three series of hydrogen the value \bar{n} of the upper state quantum number of the first merged or thin line according to the criteria just presented. Only values where the path length is an integer power of 10 have meaning. The lines were taken to be quasi-statically broadened with line width parameter w calculated from (see Part 1, Section 4.6)

$$w = 0.691 \times 10^{-2} z_r^{-1} (n_u^2 - n_l^2) (N_e / N_L + \sum z_p N_z / N_L)^{2/3}. \quad (3.1)$$

It can be seen from Fig. 8 that as the path length increases from a low value, the first thin line moves higher up the series. Then, self-absorption begins and the start of the pseudo-continuum is set by the first merged line which moves back down the series for further increases in path length.

3.4 Importance of High Lines

As an example of the method of the previous section, the intensity of some of the high lines of a hydrogenic gas was computed.

The purpose of the computation was to find for a given initial quantum number m , the upper state quantum number, n^* , such that all lines of that series with upper states higher than n^* taken together carry less than 10% of the energy in the series leading line. The calculation treated the high lines as an extension of the bound-free continuum. The leading line was assumed to be electron impact broadened with the width given by Eq. (2.8).

The calculation was carried out on a digital computer. The quantity n^* was treated as a continuous variable and found by trying successively

lower values until the correct value was straddled, after this, linear interpolation proceeded until a value which gave the desired integrated intensity to within 1% was achieved.

Before discussing the results of the calculation, certain analytical expressions which hold where the high lines are optically thin will be presented. First, suppose the leading line is also optically thin, then an expression for the ratio $I_{\text{High}}/I_{m,m+1}$ (where I_{High} is the total intensity due to all lines with $n > n^*$) can be obtained from Eq. (2.22). The procedure is to replace $m+p$ by n and integrate over n from n^* to ∞ in the manner of Appendix I. One then gets

$$\frac{I_{\text{High}}}{I_{m,m+1}} \approx \frac{(m+1)^3}{2t \exp[t/(n^*)^2]} \{ \exp[t/(n^*)^2] - 1 \}. \quad (3.2)$$

(It is clear from Appendix I that the high series contribution to Eq. (3.2) can also be obtained by integrating the optically thin emission of bound-free radiation with initial quantum number m over the photon energy interval $x_H[1/m^2 - 1/(n^*)^2]$ to x_H/m^2 .) Setting $I_{\text{High}}/I_{m,m+1} = 0.1$ and solving Eq. (3.2) for n^* yields

$$n^* = \{t/\ln[0.12t \exp[t/(m+1)^2]/(m+1)^3 + 1]\}^{1/2}. \quad (3.3)$$

Secondly, suppose the leading line is self absorbed, then we make use of the expression

$$\frac{(I_{m,m+1})_{\text{thin}}}{(I_{m,m+1})_{\text{thick}}} = \left\{ \frac{s \int_0^{\infty} K_{vm,m+1} dv^{1/2}}{4w} \right\}^{1/2} = \Gamma(m, t) s^{-1/2} \quad (3.4)$$

where

$$\bar{s} \equiv (N_e / N_L) s \quad (3.5)$$

and

$$F(m, t) \equiv 25.1 \left\{ \frac{m^3}{(m+1)(2m+1)^3} \right\}^{1/2} \exp(t/2m^2) t^{5/6} \times \left\{ 1 - \exp \left[-t \frac{2m+1}{m^2(m+1)^2} \right] \right\}^{1/2} \bar{s}^{1/2} \quad (3.6)$$

Equation (3.6) assumes an electron impact-broadened leading line with a width given by Eq. (2.8). It also assumes the number densities of ions and electrons to be equal. Combining Eqs. (3.4) and (3.2) and solving for n^* gives

$$n^* = \{t / [t n [0.12t \exp[t/(m+1)^2] / (m+1)^3 F(m, t) \bar{s}^{1/2} + 1]]\}^{1/2}. \quad (3.7)$$

For $(n^*)^2 \gg t$ Eq. (3.7) becomes

$$n^* = \{10 F(m, t) \frac{(m+1)^3}{2t} \exp[-t/(m+1)^2]\}^{1/2} \bar{s}^{1/4} \quad (3.8)$$

(the corresponding form of Eq. (3.3) is not of interest since for this case $(n^*)^2$ is not larger than t).

Figures 9a, 9b and 9c show results for $m = 1, 2$ and 3 respectively. The optically thin expression (3.3) appears as a number of horizontal lines while Eq. (3.7) gives straight (or nearly straight) lines on these figures. The intersections of these lines correspond to the point at which the treatment of the leading line changes from optically thin to self-absorbed (see Fig. 7 of Part 1). Curves obtained by numerical integration of the pseudo-continuum are shown for densities of 1 and 10^{-3} times atmospheric.

As s increases, these curves follow the optically thin results until self-absorption of the high lines causes a departure from the analytical expression. It can be seen that n^* reaches a maximum and then falls off at large values of s due to the self-absorption of the high lines. The values of n^* give an indication of the relative importance of the high lines since where n^* is large, a large number of lines have to be accounted for if errors of 10% are to be avoided.

It can be seen from Figs. 8 and 9 that in general, n^* lies above \bar{n} , the beginning of the pseudo-continuum. One implication of this is that the high lines generally transfer more than 1/10 as much energy as the leading line. For this reason, some reasonable method of accounting for the high lines has to be included in any radiative transfer calculation for a real gas.

3.5 Treatment of Lines and Photoionization from Highly Excited Lower States

Sections 3.2 and 3.3 treated lines at the end of comparatively low-lying series where a number of preceding, isolated lines exist. In this section, we follow a similar line of argument for the case of high series and bound-free transitions from highly excited states.

In Section 3.2 we saw that the merging of the high lines of a series causes an apparent extension of the bound-free continuum. Since the line-width increases with the upper state quantum number, as one passes to higher series the line merging will spread, covering more and more lines until all the lines are merged. At approximately the same condition the minimum frequency for a transition will go to zero; this behavior corresponds to perturbations of the energy levels at m and $m+1$ being so great that they overlap and the energy changes can take all values. Such a situation suggests

that transitions by highly excited electrons will be similar to those of free electrons. The following discussion shows that this is essentially true and points out certain differences.

Let us suppose that the quantum number at which the energy levels overlap is \bar{m} as predicted by the theory of either Inglis and Teller¹² or Armstrong¹³ and let us consider the absorption coefficient due to transitions between states with $m > \bar{m} \gg 1$. For any high series, since $n > \bar{m}$, the lines will be merged throughout the series and since $m > \bar{m}$ the first two levels overlap and the series extends to zero frequency. As noted previously (see Section 3.2), overlapping line profiles produce an absorption coefficient which can be closely approximated by extending the bound-free absorption coefficient to the beginning of the merged lines. In this case ($m > \bar{m}$), the bound-free absorption coefficient can thus be extended to zero frequency.

The absorption coefficient at frequency ν due to all transitions from all states with $m \geq \bar{m}$ is therefore given by:

$$K_\nu = \frac{2^5 \pi^2 e^6}{3\sqrt{3} \operatorname{ch}^4 \frac{Q}{a} h^3} \frac{z^4}{v^3} \frac{Ry}{e^{-\chi/kT}} \sum_{m=\bar{m}}^N \exp(z^2 Ry/m^2 kT) \frac{1}{m^3} (1 - e^{-hv/kT}), \quad (3.9)$$

where Ry is the Rydberg energy constant. Changing the summation to integration, Eq. (3.9) becomes

$$K_\nu = \frac{2^5 \pi^2 e^6}{3\sqrt{3} \operatorname{ch}^4 \frac{Q}{a}} \frac{z^2}{v^3} e^{-\chi/kT} \frac{N}{\bar{m}^3} kT (1 - e^{-hv/kT}) [\exp(z^2 Ry/(\bar{m})^2 kT) - 1] \quad (3.10)$$

or

$$K_\nu = K_{\nu, \text{ff}} \frac{1}{Q_i} [\exp(z^2 Ry/(\bar{m})^2 kT) - 1] \quad (3.11)$$

where $K_{v,ff}$ is the free-free absorption coefficient. In the case of hydrogen, $Q_i = 1$. It is worth observing that $z^2 Ry/(\bar{m})^2 = \Delta x$ where Δx is the distance below the threshold of the energy level corresponding to \bar{m} . The appearance of free-free-like behavior in Eq. (3.11) at all frequencies is a consequence of the free-bound absorption coefficients extending to zero and may be contrasted with the result of the corresponding integration carried out by Sibulkin¹⁴ for the true photoionization transitions. In the latter case, free-free-like behavior only exists for frequencies above a certain minimum value.

It is tempting to suggest from Eq. (3.11) that the transitions from highly excited states can be accounted for by depressing the ionization potential by Δx thus increasing the number of free electrons and reducing the number of atoms. However, if such a reduction in ionization energy is carried out in the Saha equation, the increase in the number of free electrons predicted is less than the number of atoms which previously occupied states such that $m > \bar{m}$. The explanation for this disparity is that if the ionization potential were suddenly depressed, all electrons in states with $m > \bar{m}$ would be released but, on collision with ions already present, some would recombine to form atoms.* In summary, we may say that highly excited, highly perturbed states behave like free states in their interaction with radiation (i.e. as far as their cross-sections are concerned) but the electrons are not available for collisional interaction with other particles and hence they must not be treated as free in the calculation of species concentrations. (This is in contrast to the electrons released by the Debye-Hückel

* Where the ionization is very low, there are virtually no ions available for collisions and the released electrons remain free. Under these conditions, it can be shown that a reduction of Δx in the ionization potential used in the Saha equation leads to an additional contribution to the free-free absorption coefficient equal to the expression (3.11).

effect discussed in Section 2.2 of Part 1 which are in all senses free.)

It will now be shown that Eq. (3.11) can be used to calculate the intensity from series that have no isolated, self-absorbed lines. The approach is similar to that used for the high lines of low series. Where the lines are optically thick and merged according to their equivalent widths, it has already been shown that they can be represented by an extension of the bound-free coefficient. But when the entire series is merged, this extension will go to zero frequency and can be included in the summation of Eq. (3.9). Similarly, we have shown that the radiation from optically thin lines with $n \gg 1$ and that from a corresponding section of the extended continuum is the same, a completely optically thin series can therefore be treated as entirely bound-free and if m is large may be considered to reach zero frequency with very small error, it can therefore be treated by Eq. (3.11). Now, the effective width of the leading line rises as $m^{3/5}$ whereas the interline spacing falls as m^{-3} so that once a series with completely merged leading lines has been found, all higher series whose leading lines are optically thick will also be completely merged. We can therefore use Eq. (3.11) to treat all series higher than the first which is either entirely optically thin or completely merged and satisfies $m \gg 1$.

The results of calculations of \bar{m} are presented in Fig. 10. Only values where the path length is an integer power of 10 have meaning. The lines were taken to be quasi-statically broadened with a linewidth parameter according to Eq. (3.1). As the path length increases from a low value, the number of completely thin series decreases and hence \bar{m} increases. Subsequently, \bar{m} is fixed by the first completely merged series and consequently falls with increasing path length.

3.6 Importance of Lines and Photoionization from Highly Excited Lower States

This section reports some calculations which apply the treatment of the previous section to a hydrogenic gas.

The computations were analogous to those of Section 3.4. Their purpose was to calculate m^* the lower state quantum number such that all transitions with lower states higher than m^* together carry less than 10% of the energy of the Lyman α line. Two computations of m^* were performed: one which accounted only for high series and one which accounted for high series and high photoionization (i.e. photoionization from highly excited initial states). In each case, the Lyman α line was taken to be electron impact broadened with a width given by Eq. (2.8). The intensity of the combination of high series and high photoionization was calculated by numerical integration using the continuous absorption coefficient given in Eq. (3.11) with m^* replacing \bar{m} . The intensity of the high series alone was obtained from the following absorption coefficient

$$K_v = K_{v,ff} [\exp(Ry/(m^*)^2 kT) - \exp(hv/kT)] \quad \text{for } hv < Ry/(m^*)^2 kT$$

$$K_v = 0 \quad \text{for } hv > Ry/(m^*)^2 kT. \quad (3.12)$$

Equation (3.12) may be obtained by integrating the true bound-free contributions due to states with $m > m^*$ and subtracting the result from Eq. (3.11). A trial and interpolation procedure similar to that used for the high lines (Section 3.4) was employed.

As in the case of high lines, analytic expressions can be obtained where the lines are optically thin, as follows. First, suppose the Lyman α line is optically thin. Then, starting from Eq. (2.14) we set $m' = 1$, $n' = n$, integrate n from $m+1$ to ∞ and m from m^* to ∞ . The result is

$$\frac{I_{HS}}{I_a} = 2t^{-2} \exp(-t/4) \left(\exp[t/(m^*)^2] - 1 - t/(m^*)^2 \right) \quad (3.13)$$

where I_{HS} is the total intensity due to all lines with $m > m^*$ and I_a is the intensity due to the Lyman α line. Setting $I_{HS}/I_a = 0.1$, Eq. (3.13) can be written

$$m^* = \{t/\ln[0.05t^2 \exp(t/4) + 1 + t/(m^*)^2]\}^{1/2} \quad (3.14)$$

which can be solved by iteration, starting with $t/(m^*)^2 = 0$. A similar procedure can be applied to the case of combined high series and high photoionization, yielding

$$m^* = \{t/\ln[0.05t^2 \exp(t/4) + 1]\}^{1/2}. \quad (3.15)$$

Secondly, if the Lyman α line is self-absorbed, Eq. (3.4) must be introduced, yielding for high series the relation

$$m^* = \{t/\ln[1.47 \times 10^{-2} t^{7/6} e^{-t/4} (1-e^{-3t/4})^{-1/2} \bar{s}^{-1/2} + 1 + t/(m^*)^2]\}^{1/2} \quad (3.16)$$

where $\bar{s} \equiv sN_e/N_L$. For $m^* \gg t$ Eq. (3.16) becomes

$$m^* = 2.42 e^{t/16} t^{5/24} [(1-e^{-3t/4}) \bar{s}]^{1/8}. \quad (3.17)$$

The result for high series and high photoionization corresponding to Eq. (3.16) is

$$m^* = \{t/\ln[1.47 \times 10^{-2} t^{7/6} e^{-t/4} (1-e^{-3t/4})^{-1/2} \bar{s}^{-1/2} + 1]\}^{1/2}. \quad (3.18)$$

For $m^* \gg t$ Eq. (3.18) becomes

$$m^* = 8.33 e^{t/8} t^{-1/12} (1-e^{-3t/4})^{1/4} \bar{s}^{-1/4}. \quad (3.19)$$

Figures 11 and 12 show results for high series and high series plus high photoionization respectively. Equations (3.14) and (3.15) give horizontal straight lines for each temperature but these only appear within the range of values considered at $t = 4$. Equations (3.16) and (3.18) give straight (or nearly straight) lines on these figures. The intersection of lines from Eq. (3.16) or (3.18) with the line at the same temperature given by Eq. (3.14) or (3.15), as appropriate, corresponds to the point at which the Lyman α line changes from being optically thin to self-absorbed (see Fig. 7 of Part 1). Curves obtained by the numerical integration procedure outlined previously are shown for densities of 1 and 10^{-3} times atmospheric. As s increases, these curves follow the optically thin results until self-absorption of the high transitions sets in. This self-absorption causes m^* to pass through a maximum in the case of the high series alone but for high series and high bound-free, m^* is sufficiently high that the transitions remain nearly optically thin for all cases presented. Figures 11 and 12 show that m^* can reach considerable values.

Comparing Fig. 10 with Figs. 11 and 12 shows that in most cases m^* lies above \bar{m} implying that the high series usually transfer at least 1/10 as much energy as the Lyman α line.

APPENDIX I. Optically Thin Radiation from High Lines and the Bound-Free Continuum

The intensity from an optically thin line corresponding to a transition $m \rightarrow n$ in an ion of charge $z-1$ is (see Section 3.1)

$$I_{mn} = \frac{\pi e^2}{m c} N_m f_{mn} B_{v_{mn}} [1 - e^{-hv_{mn}/kT}] s.$$

Substituting the Boltzmann relation, Eq. (2.5), the hydrogenic expression for f_{mn} and the explicit form of the Planck function we get

$$I_{mn} = \frac{2^9 \pi^4 m_e^4 e^{10} z^6}{3\sqrt{3} c^3 h^6} \frac{\chi_H}{m^3} \frac{N}{Q_a} e^{-\chi_H/kT} s \frac{1}{n^3} e^{z^2 \chi_H/n^2 kT}. \quad (I.1)$$

The total intensity from lines lying in the interval $n_1 \leq n \leq n_2$ is found by summing Eq. (I.1) over n . Changing the summation to integration (which implies $n_1 \gg 1$) gives

$$\sum_{n=n_1}^{n_2} I_{mn} \approx \frac{2^8 \pi^4 m_e^4 e^{10} z^4}{3\sqrt{3} c^3 h^6} \frac{1}{m^3} \frac{N}{Q_a} e^{-\chi_H/kT} kT s [\exp(z^2 \chi_H/n_1^2 kT) - \exp(z^2 \chi_H/n_2^2 kT)]. \quad (I.2)$$

Now, since the photon energy can be expressed as

$$hv = \chi_H - z^2 \chi_H/n^2 - E_m,$$

Eq. (I.2) may be written

$$\sum_{n=n_1}^{n_2} I_{mn} \approx \frac{2^8 \pi^4 m_e^4 e^{10} z^4}{3\sqrt{3} c^3 h^6} \frac{1}{m^3} \frac{N}{Q_a} e^{-E_m/kT} kT s [e^{-hv_1/kT} - e^{-hv_2/kT}] \quad (I.3)$$

where v_1 and v_2 are the central frequencies of lines with lower state m and upper states n_1 and n_2 respectively.

The optically thin emission from a bound-free continuum with initial state m in the interval v_1 to v_2 is

$$\begin{aligned}
 I_{bf} &= \int_{v_1}^{v_2} B_v \sigma_{v,m} N_m dv \\
 &= \frac{2^8 \pi^4 m e^{10} z^4}{3\sqrt{3} c^3 h^5} \frac{1}{m^3} \frac{N_a}{Q_a} e^{-\Sigma_m/kT} s \int_{v_1}^{v_2} e^{-hv/kT} dv
 \end{aligned} \tag{I.4}$$

which gives

$$I_{bf} = \frac{2^8 \pi^4 m e^{10} z^4}{3\sqrt{3} c^3 h^6} \frac{1}{m^3} \frac{N_a}{Q_a} e^{-\Sigma_m/kT} \frac{kT}{s} [e^{-hv_1/kT} - e^{-hv_2/kT}] \tag{I.5}$$

Finally, comparing Eqs. (I.3) and (I.5) we find that $I_{bf} = \sum_{n=n_1}^{n_2} I_{mn}$.

APPENDIX II. The Use of the Bound-Free Continuum Absorption Coefficient to Represent Self-Absorbed, Effectively Merged High Lines

Self-absorbed, effectively merged high lines radiate with black-body intensity at all frequencies of the interval over which they occur. Such lines can therefore be replaced by any continuous absorption coefficient which is large enough to give black-body radiation in the appropriate interval. It is the purpose of this Appendix to show that the extrapolated bound-free absorption coefficient is sufficiently large in the above sense. We do this by showing that the minimum value of the optical depth of the extended continuum corresponding to merged, self-absorbed lines is sufficiently large to give approximately black-body radiation.

The lines which we consider are assumed to have the asymptotic wing profile $L(v) = b/(v-v_0)^a$ (see Part 1, Section 3.3) where b and a can vary from line to line. Certain useful relationships for such lines have been derived in Part 1, Section 3.3 and will be repeated here for convenience. The line is considered as either optically thin or self-absorbed depending on the optical depth τ defined by

$$\tau = \left(\int_0^{\infty} K_v dv / w \right) s = \frac{\pi e^2}{m_e c} f N s / w [1 - \exp(-hv/kt)] \quad (II.1)$$

where N is the number density of particles in the initial state and w is a line width parameter given by

$$w = b^{1/(a-1)} \left[\Gamma(1 - \frac{1}{a}) \right]^{a/(a-1)}. \quad (II.2)$$

The separation between optically thin and self-absorbed behavior is defined to be at

$$\tau = 2^{a/(a-1)}. \quad (\text{II.3})$$

When optically thin, the effective width is given by

$$W = w\tau. \quad (\text{II.4})$$

When self-absorbed, the effective width is given by

$$W = 2w \tau^{1/a}. \quad (\text{II.5})$$

Our first step is to use the above equations to find the optical depth at a distance of half the effective width from the line center (i.e. at $v_W \equiv v_0 \pm W/2$) when the line is self-absorbed. Using the standard relationship between the normalized line profile and the absorption coefficient at a point in the line, we get for the optical depth at v_W

$$\tau_{v_W, L} = K_{v_W, L} s = \int_0^\infty K_{v, L} dv \ L(v_W) s.$$

Inserting into this the expression for $L(v)$ and Eq. (II.1) we obtain

$$\tau_{v_W, L} = w\tau b/(W/2)^a. \quad (\text{II.6})$$

Finally, Eqs. (II.2), (II.5) and (II.6) yield the simple result

$$\tau_{v_W, L} = [\Gamma(1 - \frac{1}{a})]^{-a}.^* \quad (\text{II.7})$$

Having obtained this convenient expression for optical depth at v_W , we next seek to compare the value of the continuum absorption coefficient at the line

^{*}The value of $\tau_{v_W, L}$ for $a = 2$ (dispersion profile) is $1/\pi$ while the value for $a = 2.5$ (quasi-static profile) is $1/2.7$.

frequency to the line absorption coefficient at v_w and hence, using Eq. (II.7), determine the optical depth of the continuum at the frequency of the line.

First, we ask under what conditions will the optical depth of the extended continuum be a minimum, consistent with the line to which it corresponds being both self-absorbed and merged. This question is most easily answered if we transform it into a problem in terms of the line absorption coefficient. We may do this as follows. For N particles per unit volume, the optical depth of the continuum may be written $\tau_{v,c} = N\sigma_{v,c}s$ where $\sigma_{v,c}$ is the continuum absorption cross section which is independent of temperature and density. Thus, $\tau_{v,c}$ is a minimum when Ns is a minimum. On the other hand, the line optical depth at v_w may be written, from Eq. (II.7), $\tau_{v_w,L} = N\sigma_{v_w,L}s = \text{constant}$ where $\sigma_{v_w,L}$ may vary because of the variable line width. From this last result, Ns will be a minimum when $\sigma_{v_w,L}$ is a maximum. Thus our preliminary problem has become that of finding under what conditions the line absorption cross section at the equivalent width (i.e. at v_w) has its maximum value consistent with self-absorption and merging.

This maximum value will occur when the line is simultaneously just self-absorbed and just merged as will now be argued. The line must be just self-absorbed because any greater self-absorption will increase the effective width and thus push v_w further into the wings of the line with a consequent decrease in the line absorption cross section at v_w . To see that the line must also be just merged we first observe that further merging, while remaining just self-absorbed can only be achieved by an increase in line width, w , (in order to increase w at constant τ , see Eq. (II.5)) with a compensating increase in the value of Ns (in order to maintain τ constant for increasing w , see Eq. (II.1)). Now, the optical depth at v_w

is constant (see Eq. (II.7)) and hence, since N_s has increased, the absorption cross section at v_w must have decreased.

It follows that if the extended continuum absorption coefficient gives approximately black-body radiation at the frequency of a line that is just self-absorbed and just merged, it will also give black-body radiation whenever the lines are self-absorbed and merged. We therefore examine the optical depth of the continuum in this worst case of a just self-absorbed and just merged line.

When a line is just self-absorbed, the effective width is given by combining Eqs. (II.3) and (II.5) to get

$$w = w 2^{a/(a-1)} \quad (II.8)$$

Hence, the line coefficient at one half the equivalent width from the line center is given by

$$K_{v_w, L} = \frac{\pi e^2}{m_e c} f N_m [1 - \exp(-hv_w/kT)] \frac{b}{w 2^{a/(a-1)}} \quad (II.9)$$

where we have put $v_w - v_o = w/2$ and then used Eq. (II.8). The relationship between b and w is given in Eq. (II.2). Inverting Eq. (II.2) and substituting for b in Eq. (II.9) yields

$$K_{v_w, L} = \frac{\pi e^2}{m_e c} f N_m [1 - \exp(-hv_w/kT)] \frac{[\Gamma(1 - \frac{1}{a})]^{-a}}{w 2^{a/(a-1)}}. \quad (II.10)$$

Inserting the hydrogenic expression for f (Eq. (2.7)), we get

$$K_{v_w, L} = \frac{2^6}{3\sqrt{3}} \frac{e^2}{m_e c} \frac{1}{g_m} \frac{1}{m^3} \frac{1}{n^3} \frac{c^3 R^3}{v_o^3} [1 - \exp(-hv_w/kT)] N_m \times \frac{[\Gamma(1 - \frac{1}{a})]^{-a}}{w 2^{a/(a-1)}}. \quad (II.11)$$

The hydrogenic bound-free absorption coefficient is

$$K_{v, c} = \frac{2^5}{3\sqrt{3}} \frac{e^2}{m_e c h} \frac{1}{g_m} \frac{1}{m^3} \frac{c^2 R^2}{v^3} [1 - \exp(-hv/kT)] N_m. \quad (II.12)$$

Putting $v_w = v_o = v$ in Eq. (II.11) and dividing Eq. (II.12) by the result we get

$$\frac{K_{v,c}}{K_{v,L}} = \frac{2^{a/(a-1)} n^3 w [\Gamma(1 - \frac{1}{a})]^a}{2hcR} . \quad (\text{II.13})$$

But the interline spacing, D , is given by

$$\begin{aligned} D &= cRh[1/n^2 - 1/(n+1)^2] \\ &\approx cRh 2/n^3 \end{aligned} \quad (\text{II.14})$$

(since $n \gg 1$) and where lines are just starting to merge, $w 2^{a/(a-1)} = w = D$ so that Eq. (II.13) and (II.14) can be combined to give

$$\frac{K_{v,c}}{K_{v,L}} = [\Gamma(1 - \frac{1}{a})]^a . \quad (\text{II.15})$$

Finally, since $\tau_v = K_v s$, we combine Eqs. (II.15) and (II.7) to obtain the optical depth of the continuum,

$$\tau_{v,c} = 1. \quad (\text{II.16})$$

The interpretation of Eq. (II.16) in terms of a specific intensity is straightforward since in a uniform medium with no incident radiation we have (see Part 1, Section 3.1)

$$I_v = B_v (1 - e^{-\tau_v}) . \quad (\text{II.17})$$

It therefore turns out that at the frequency of a line which is just self-absorbed and just merged, use of the pseudo-continuum absorption coefficient gives 63% of black-body radiation. Since the case examined is on the

borderline between self-absorption and non-self-absorption^{*}, this value of intensity should be close to the true value. Under conditions where the lines are more heavily self-absorbed and/or further merged, use of the corresponding extended bound-free absorption coefficient will give an intensity closer to the black-body value.

* It should be remarked that whereas the lines are considered either self-absorbed or non-self-absorbed in our simplified model, no absolute distinction is made for the continuum. The pseudo-continuum may therefore be said to have correctly reproduced the partially self-absorbed condition of a more accurate line model.

APPENDIX III. Self-Absorption of the Extended Continuum Corresponding to Optically Thin Lines

In order to be able to represent optically thin lines by an extension of the bound-free absorption coefficient (see Section 3.3) it is necessary that where the lines are optically thin, then the extended continuum should also be approximately optically thin.

To start the discussion, we have to consider a situation in which we know the optical depth of the continuum. Appendix II demonstrates that, in the case of a line which is just optically thick (and hence also just optically thin) and whose equivalent width equals the interline spacing, then the optical depth of the corresponding bound-free continuum is unity. In this case, therefore, the continuum is partly self-absorbed. If the path length is decreased for constant line width then the line will become thinner while the continuum will also become thinner. If the line width and path length are decreased at the same rate the line will remain just optically thin but the continuum will become thinner. The final possibility is to increase the line width and path length keeping the line just optically thin. The increasing path length will increase the self-absorption of the continuum, apparently making the representation worse. However, we recall that we start with a line whose equivalent width is equal to the interline spacing. Increasing the width of the absorption coefficient of such a line will cause it to more heavily overlap its neighbors with a mutual increase in line absorption coefficients (except near the line centers). The line is therefore no longer necessarily thin and must be described by taking into account the mutual interference with adjacent lines. According to Section 3.2, the combined absorption coefficients of these merged lines tend towards the extended bound-free absorption coefficient.

It can thus be seen that the bound-free absorption coefficient will give a good approximation to the frequency integrated intensity from high lines wherever these lines are optically thin.

References for Part 2

1. J. S. Gruszczynski and W. R. Warren, Jr., "Study of Equilibrium Air Total Radiation," AIAA 3rd Aerospace Sciences Meeting, New York, 1966.
2. R. A. Allen, "Air Radiation Graphs: Spectrally Integrated Fluxes Including Line Contributions and Self Absorption," AVCO-Everett Research Laboratory Research Report 230 (1965).
3. L. M. Liberman, V. S. Vorobyov and G. E. Norman, "Energy Emitted in Spectral Lines by a Plasma at Equilibrium," Opt. Spectry. 14, 176-179 (1963).
4. V. S. Vorobyov and G. E. Norman, "Energy Radiated in Spectral Lines by an Equilibrium Plasma II," Opt. Spectry. 17, 96-101 (1964).
5. D. B. Olfe, "Equilibrium Emissivity Calculations for a Hydrogen Plasma at Temperatures up to 10,000°K," J. Quant. Spectrosc. Radiat. Transfer 1, 104-134 (1961).
6. H. Aroeste and W. C. Benton, "Emissivity of Hydrogen Atoms at High Temperatures," J. App. Phys. 27, 117-121 (1956).
7. D. H. Menzel and C. L. Peteris, "Absorption Coefficients and Hydrogen Line Intensities," Mon. Not. Roy. Astron. Soc. 96, 77-111 (1935).
8. H. Margenau and M. Lewis, "Structure of Spectral Lines from Plasmas," Rev. Mod. Phys. 31, 569-615 (1959).
9. J. C. Stewart and K. D. Pyatt, "Theoretical Study of Optical Properties," Air Force Weapons Center, AFSWC-TR-61-71 (1961).
10. A. Pannekoek, "The Hydrogen Lines Near the Balmer Limit," Mon. Not. Roy. Astron. Soc. 98, 604-709 (1938).

11. C.-R. Vidal, "Determination of Electron Density from Line Merging," *Jl. Quant. Spectrosc. Radiat. Transfer* 6, 461-477 (1966).
12. D. R. Inglis and E. Teller, "Ionic Depression of Series Limits in One-Electron Spectra," *Astrophys. Jl.* 90, 439-448 (1939).
13. R. H. Armstrong, "Apparent Positions of Photoelectric Edges and the Merging of Spectrum Lines," *Jl. Quant. Spectrosc. Radiat. Transfer* 4, 207-214 (1964).
14. M. Sibulkin, "Absorption and Emission Characteristics of an Ideal Radiating Gas," Brown University Division of Engineering report Nonr(562)35/7 (1965).

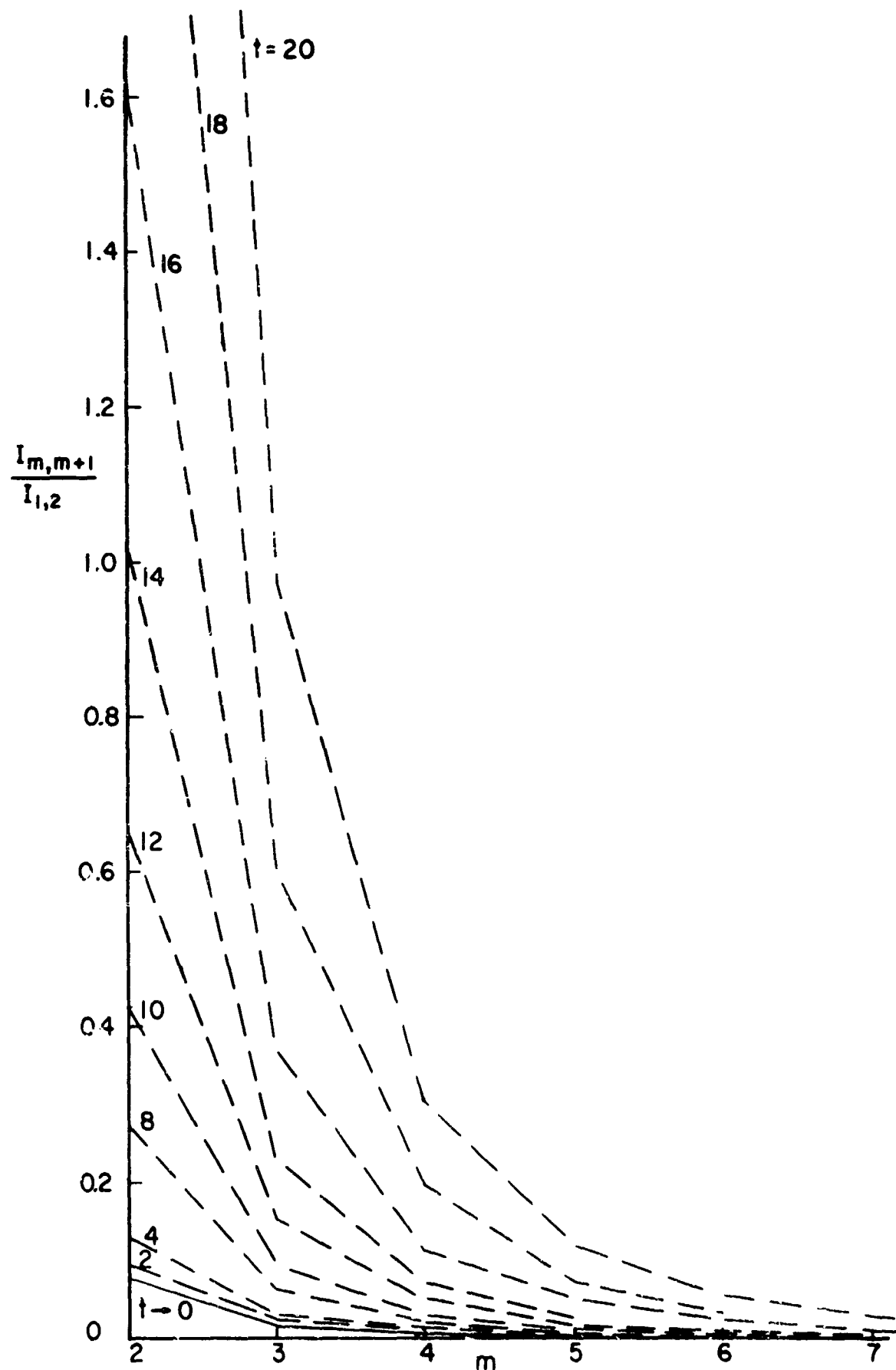


FIG. 1 INTENSITY OF LEADING LINE RELATIVE TO RESONANCE LINE AS A FUNCTION OF LOWER STATE QUANTUM NUMBER AND INVERSE TEMPERATURE PARAMETER FOR SELF ABSORBED LINES.

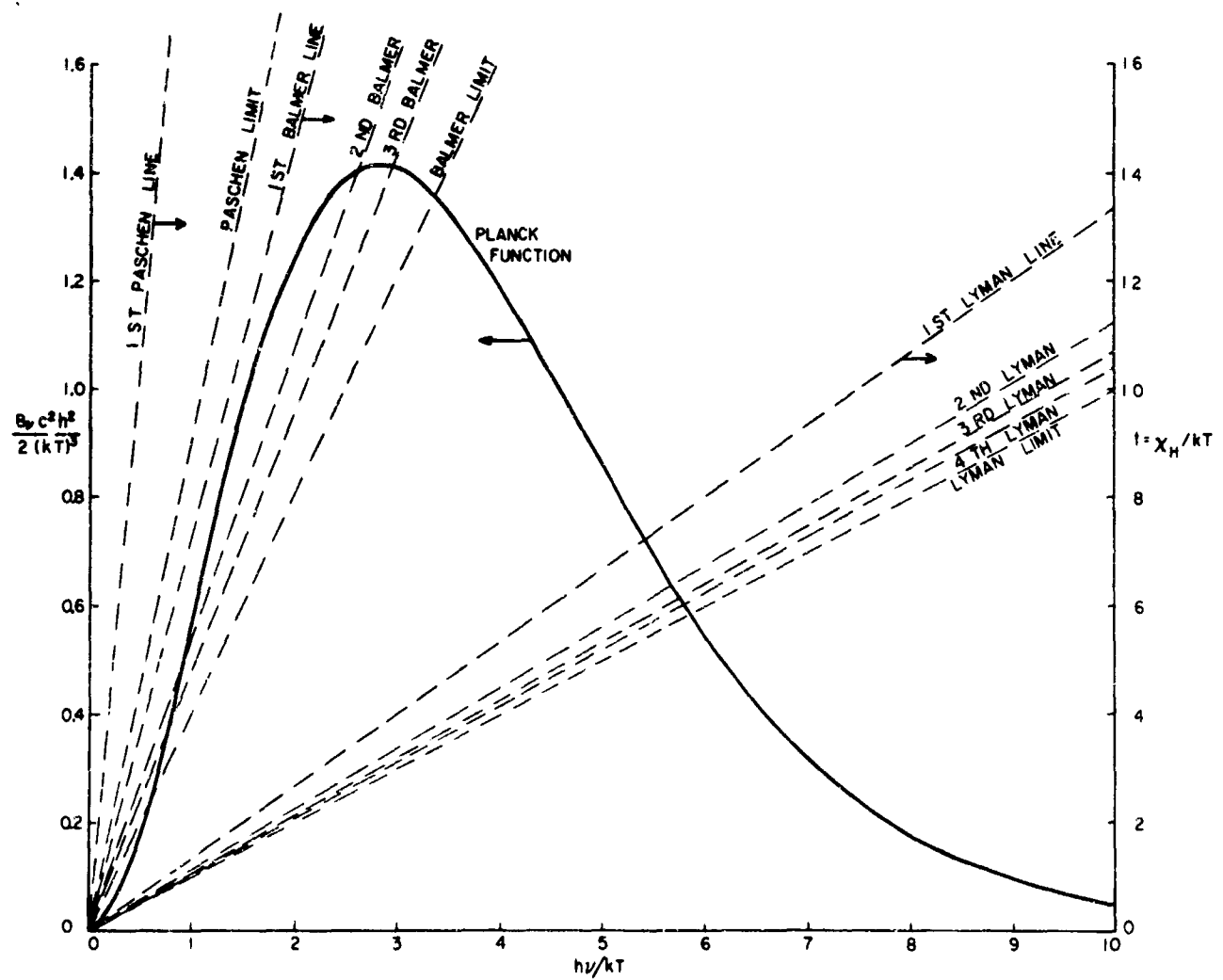


FIG. 2 PLANCK BLACK-BODY FUNCTION AND THE RELATIVE POSITIONS OF SEVERAL STRONG LINES.

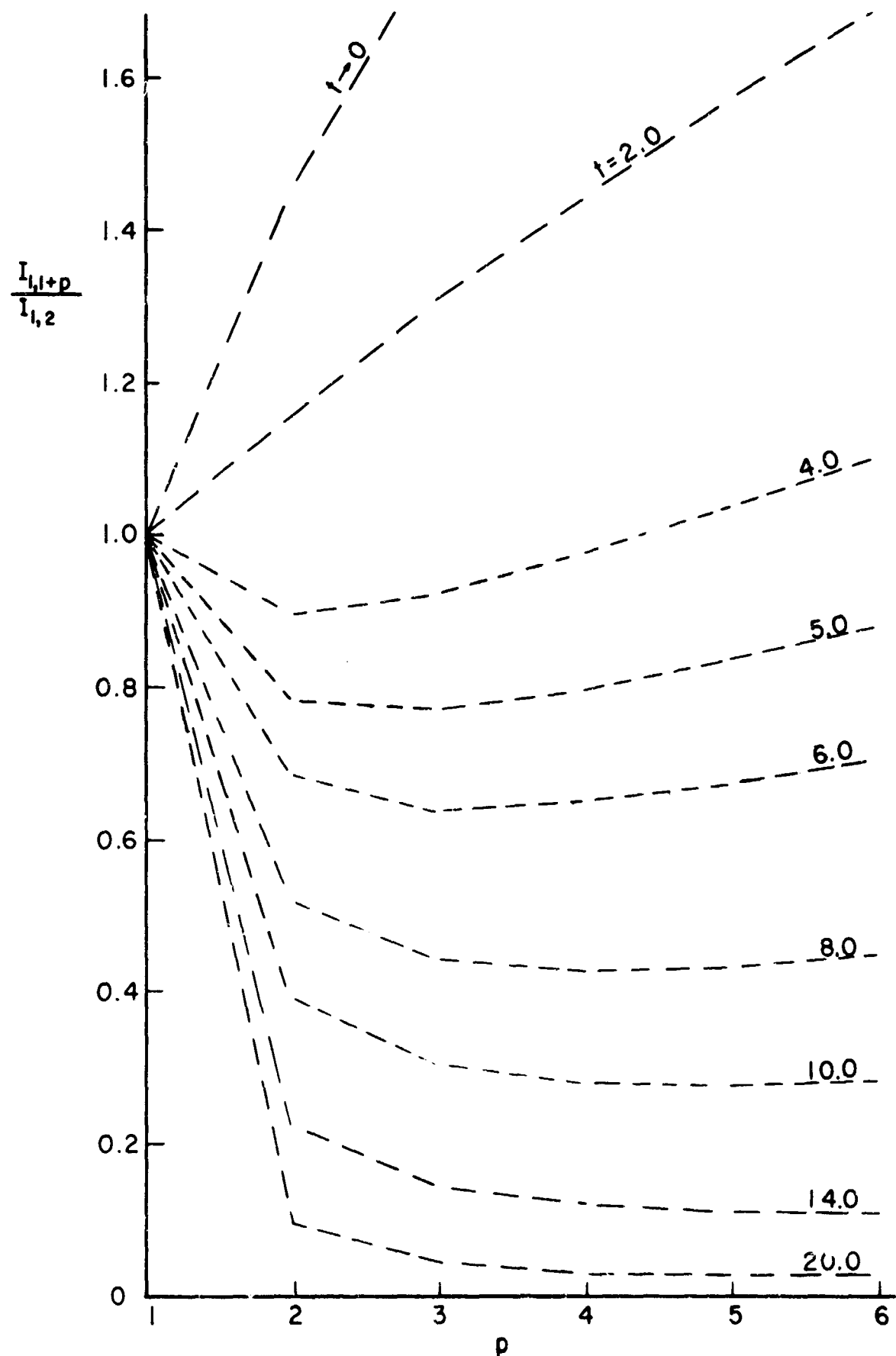
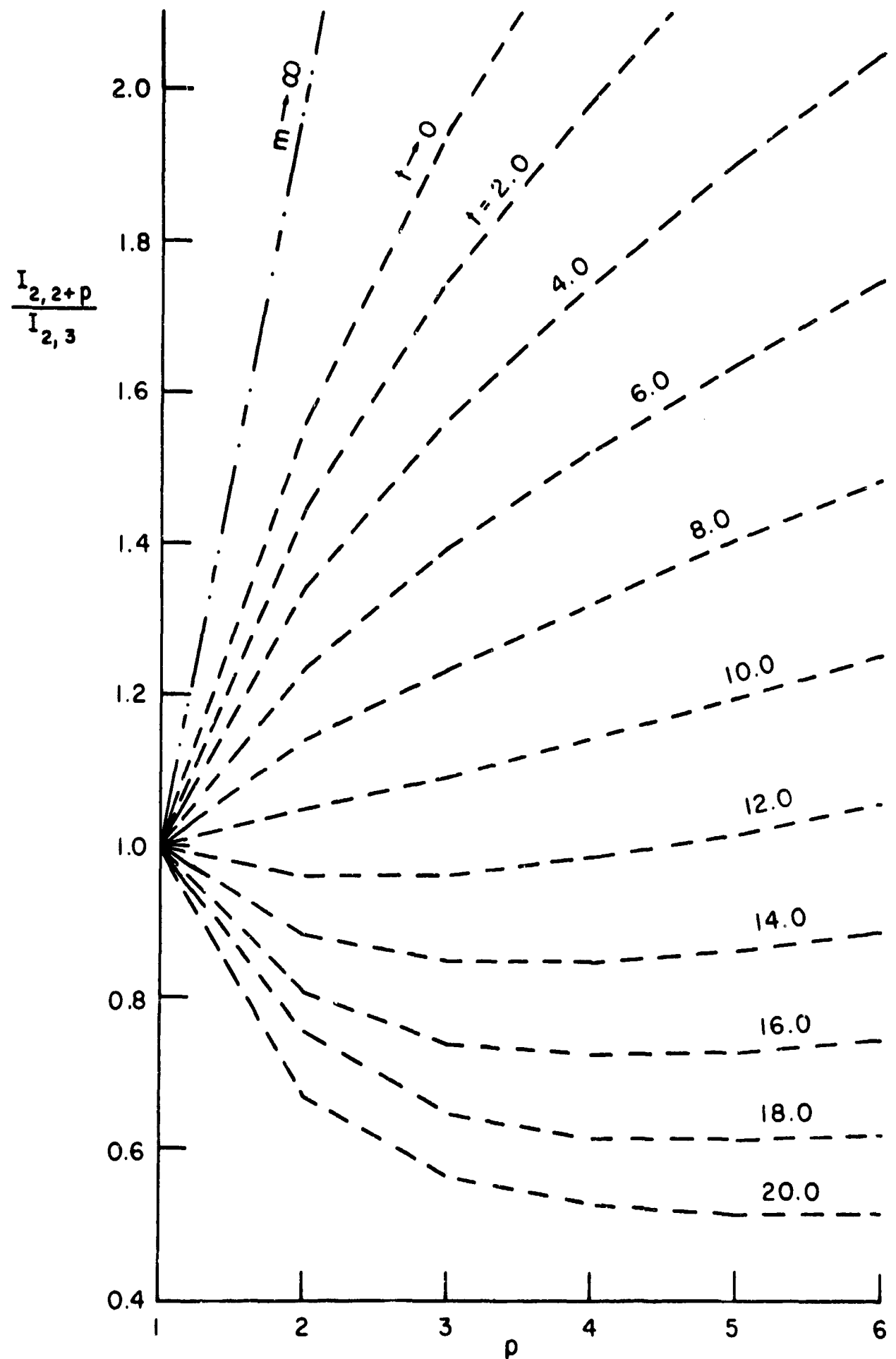
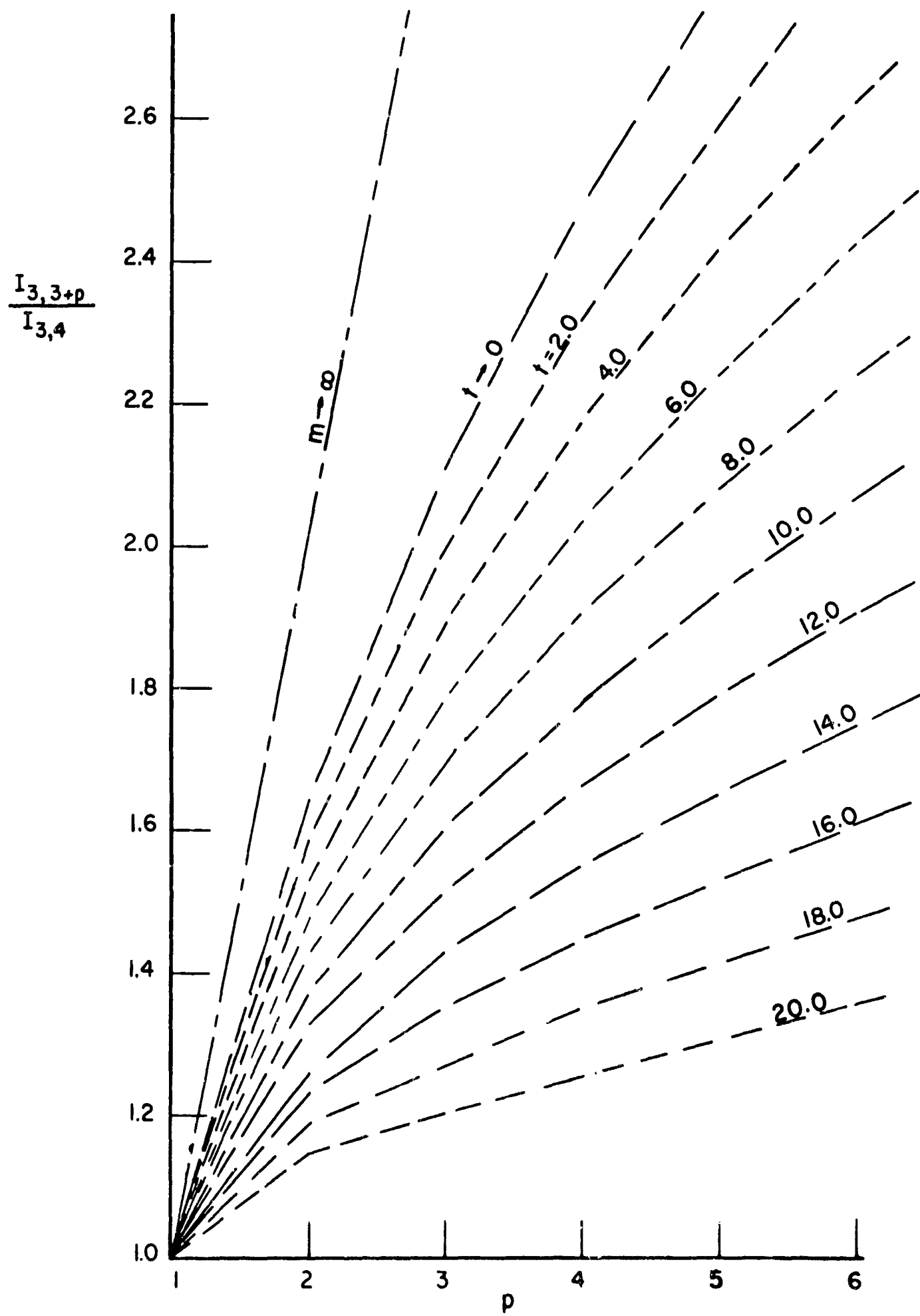


FIG. 3a LINE INTENSITY RELATIVE TO LEADING LINE INTENSITY AS A FUNCTION OF UPPER STATE QUANTUM NUMBER AND INVERSE TEMPERATURE PARAMETER FOR SELF-ABSORBED LINES.
 $m=1$

FIG. 3b $m=2$

FIG. 3c $m = 3$

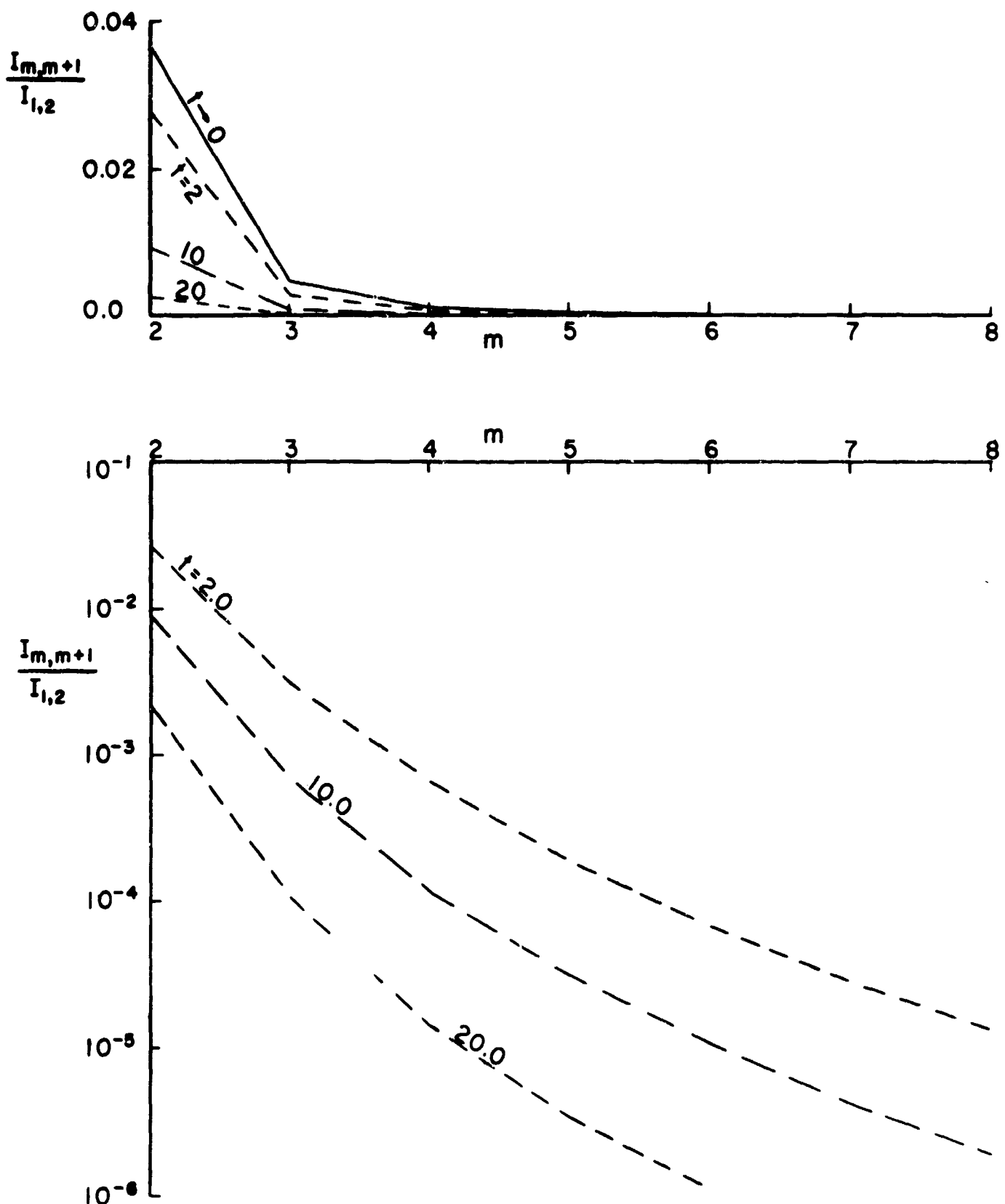


FIG. 4 INTENSITY OF LEADING LINE RELATIVE TO RESONANCE LINE AS A FUNCTION OF LOWER STATE QUANTUM NUMBER AND INVERSE TEMPERATURE PARAMETER FOR NONABSORBED LINES.

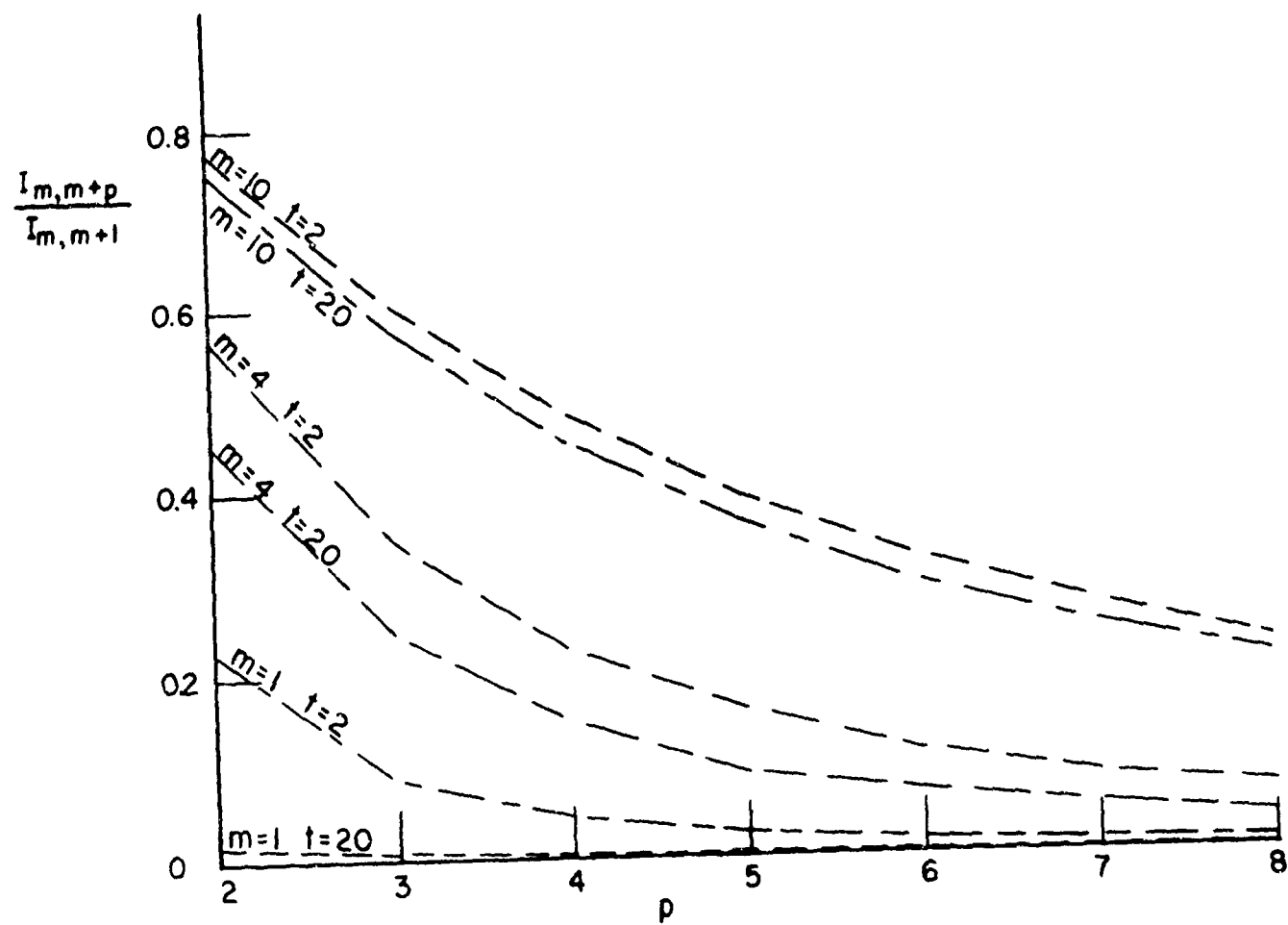


FIG. 5 LINE INTENSITY RELATIVE TO LEADING LINE INTENSITY AS A FUNCTION OF UPPER STATE QUANTUM NUMBER AND INVERSE TEMPERATURE PARAMETER FOR NONABSORBED LINES.

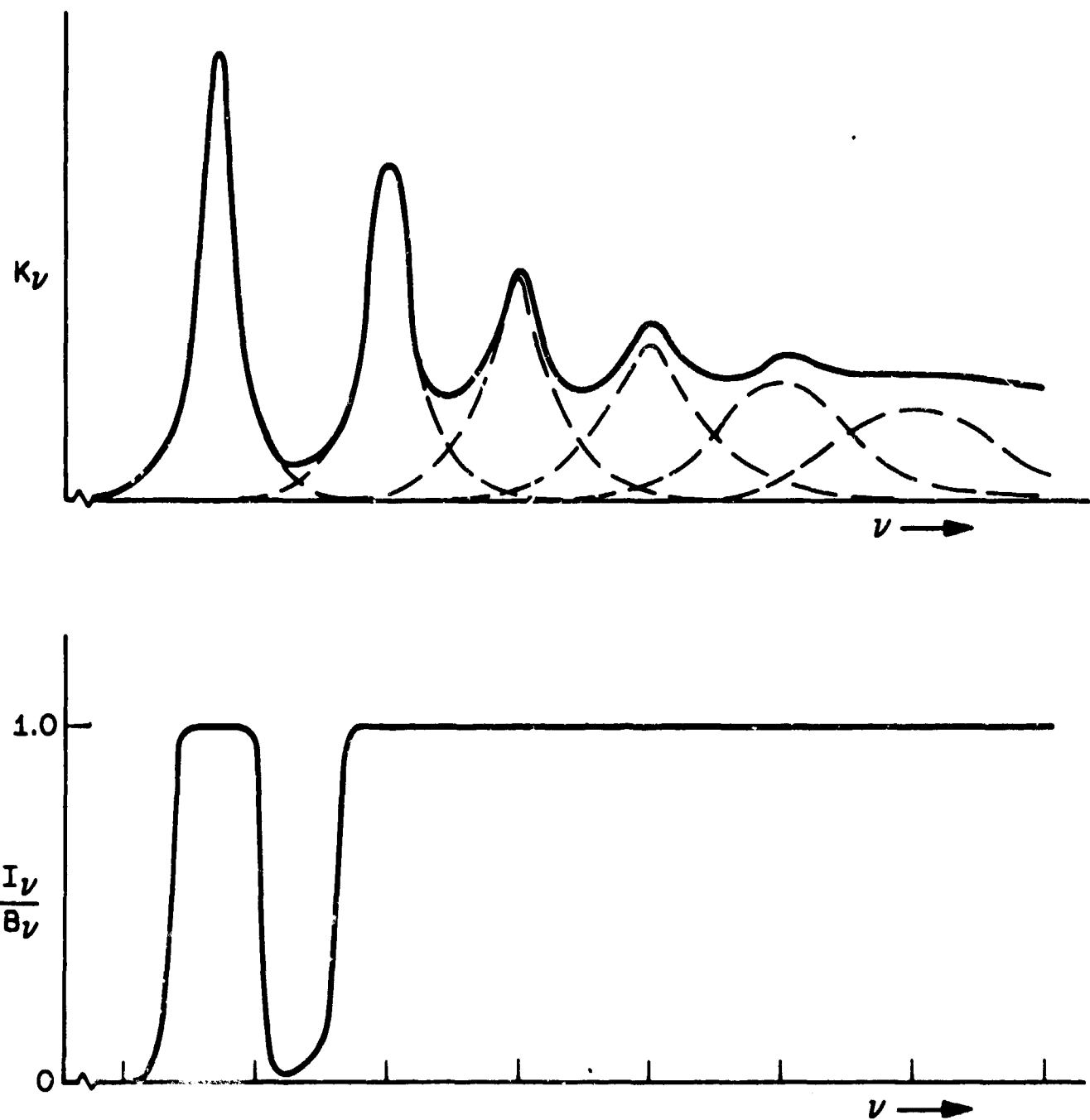


FIG. 8 SKETCH COMPARING INTENSITY PROFILES WITH ABSORPTION COEFFICIENT PROFILES FOR A SERIES OF LINES IN WHICH A SELF-ABSORBED, ISOLATED LINE IS FOLLOWED BY SEVERAL EFFECTIVELY MERGED LINES

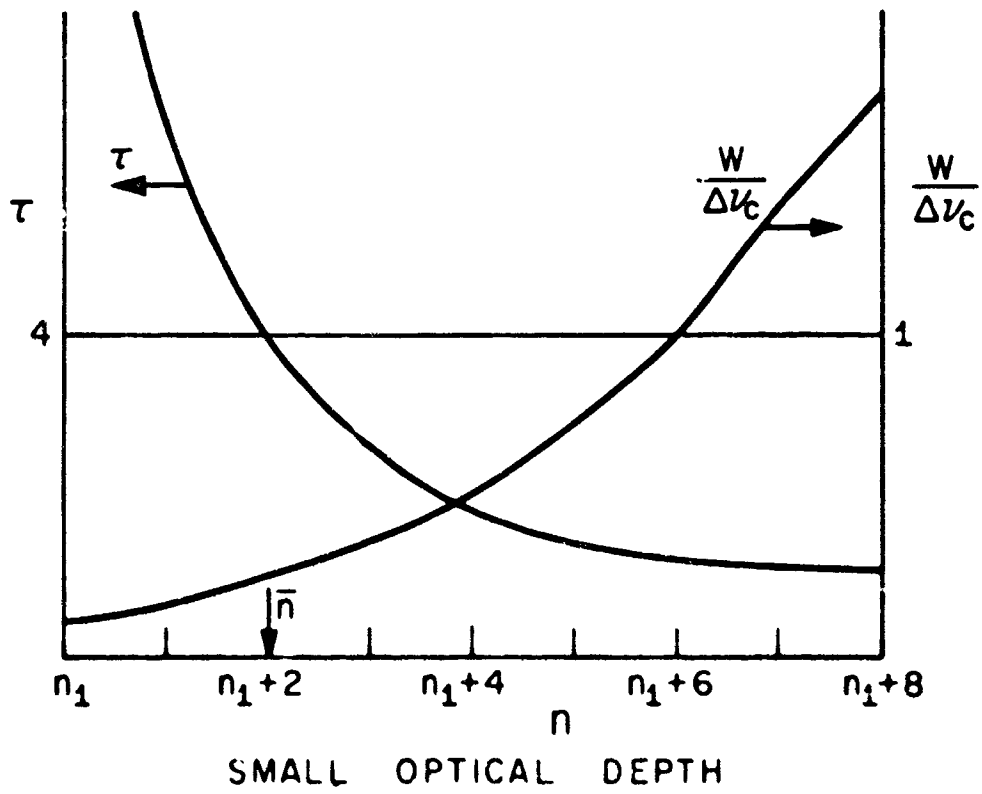
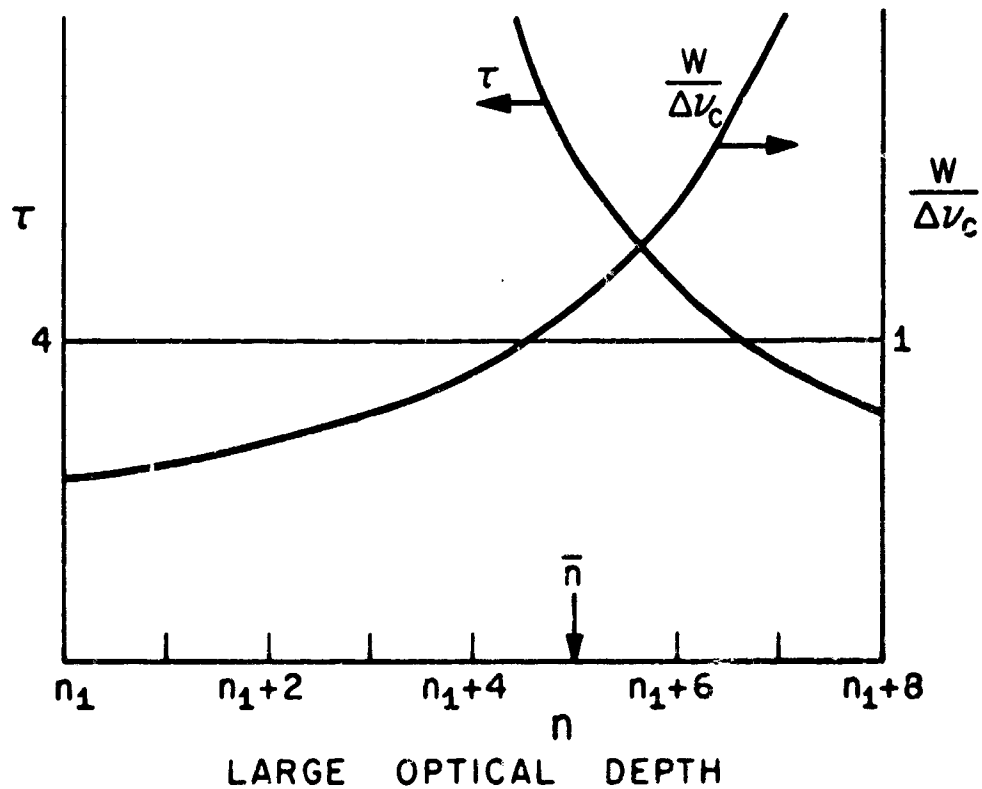


FIG. 7 SCHEMATIC ILLUSTRATION OF THE BEHAVIOR OF THE OPTICAL DEPTH AND THE RATIO OF EFFECTIVE LINE WIDTH TO INTERLINE SPACING FOR THE HIGH LINES OF A SERIES

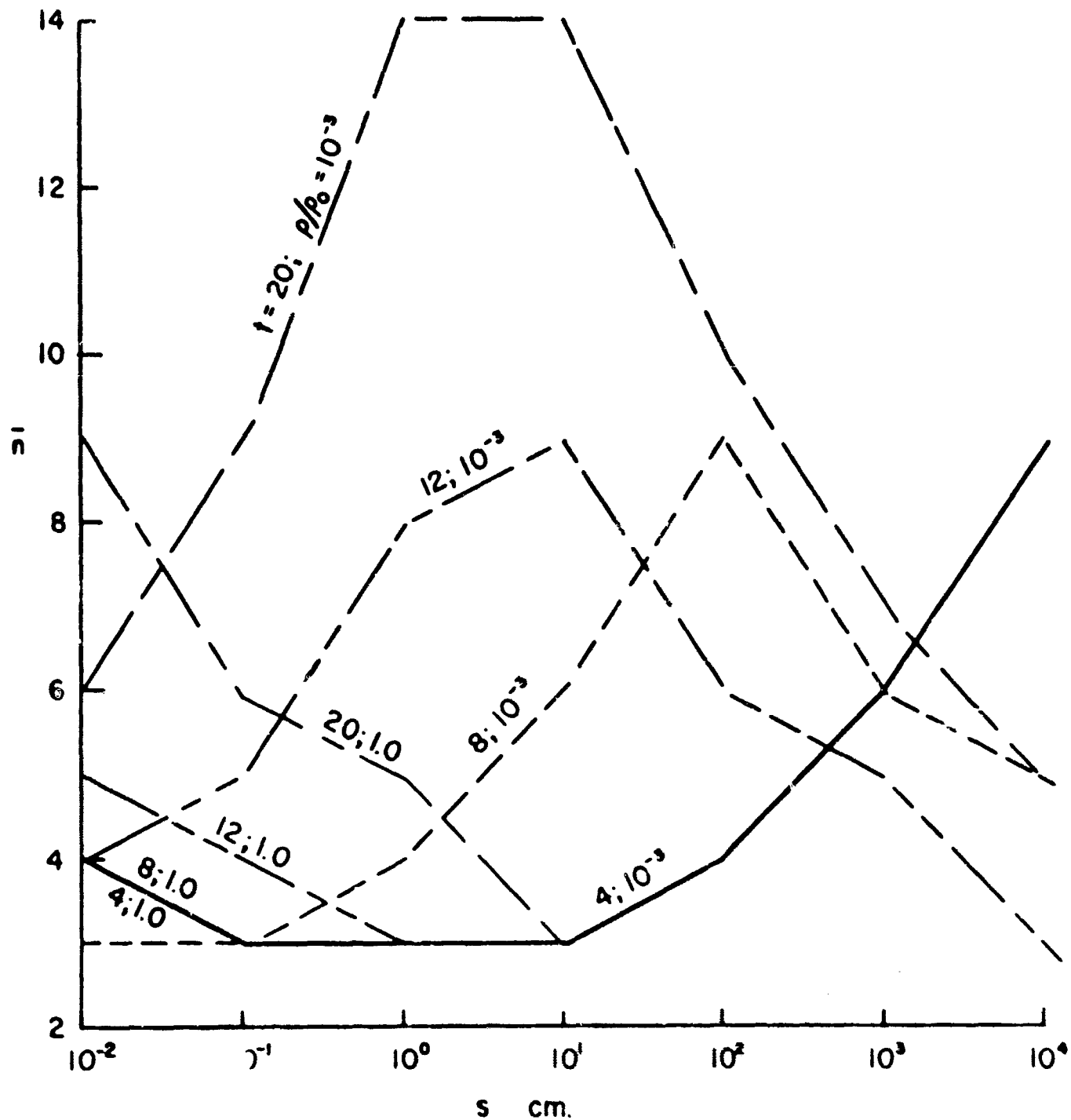
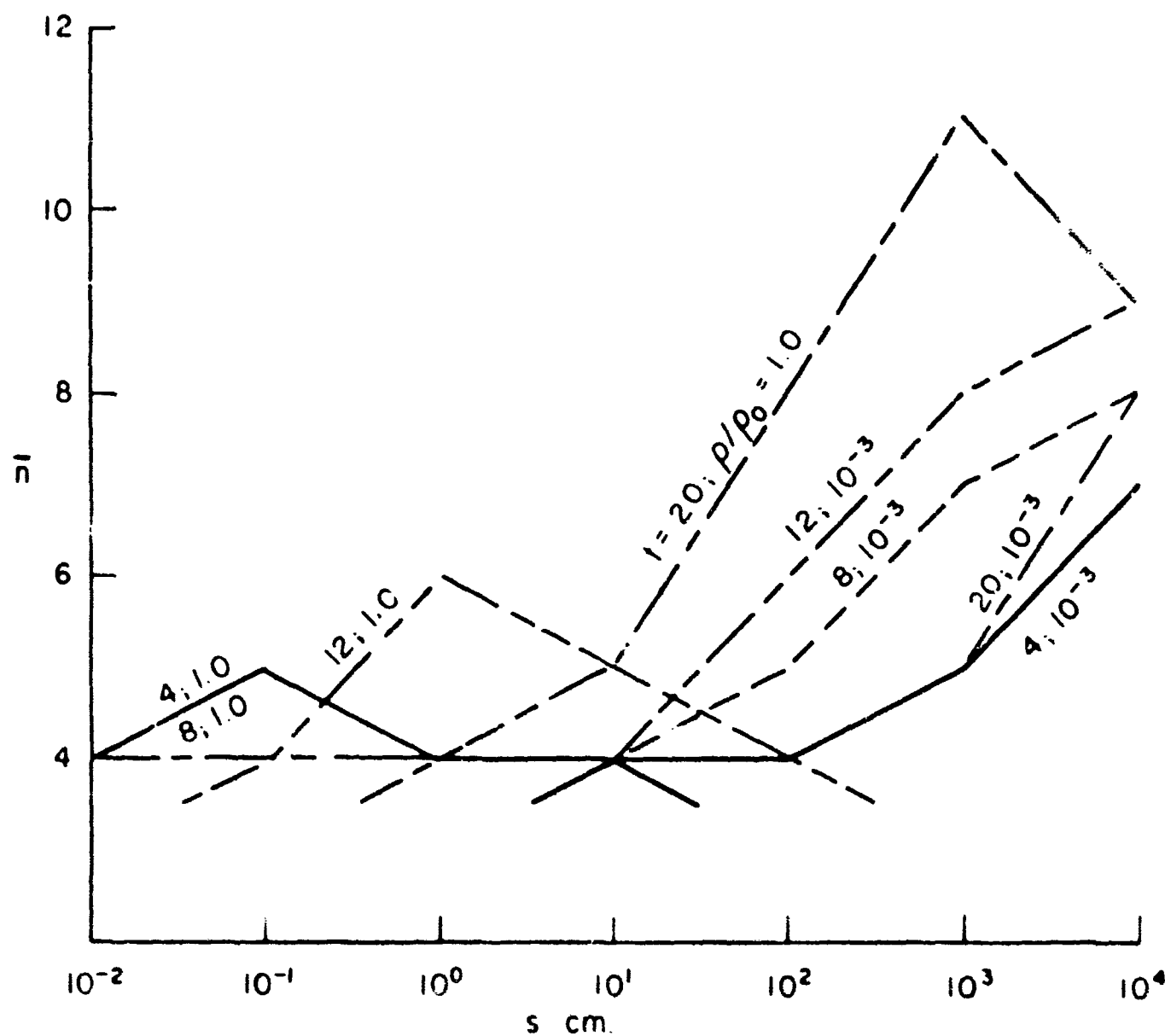
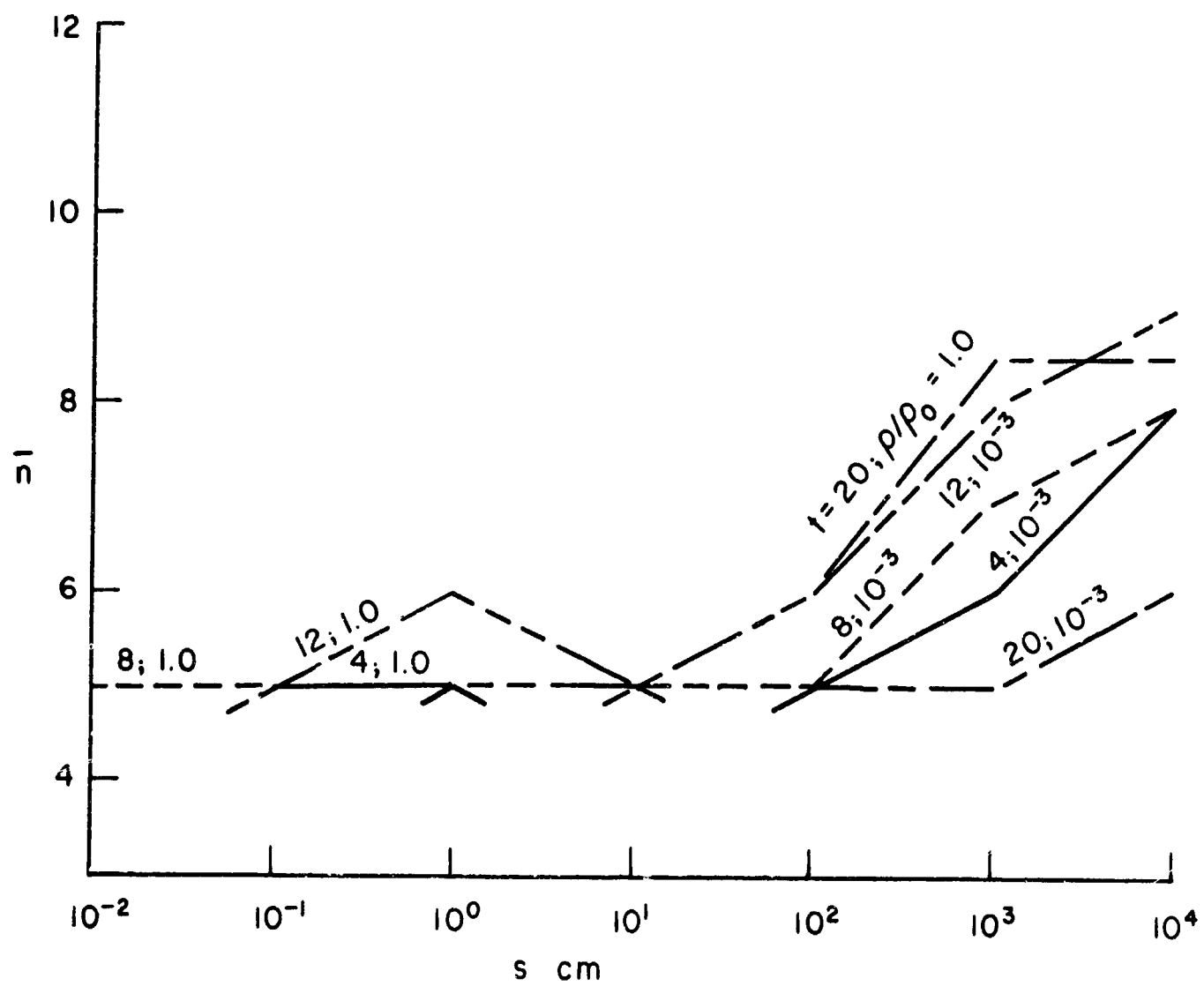


FIG. 8a UPPER STATE QUANTUM NUMBER OF FIRST MERGED OR THIN LINE.

ONLY VALUES FOR WHICH THE PATH LENGTH IS AN INTEGER POWER OF 10 HAVE MEANING.

$m = 1$

FIG. 8b $m = 2$

FIG. 8c $m = 3$

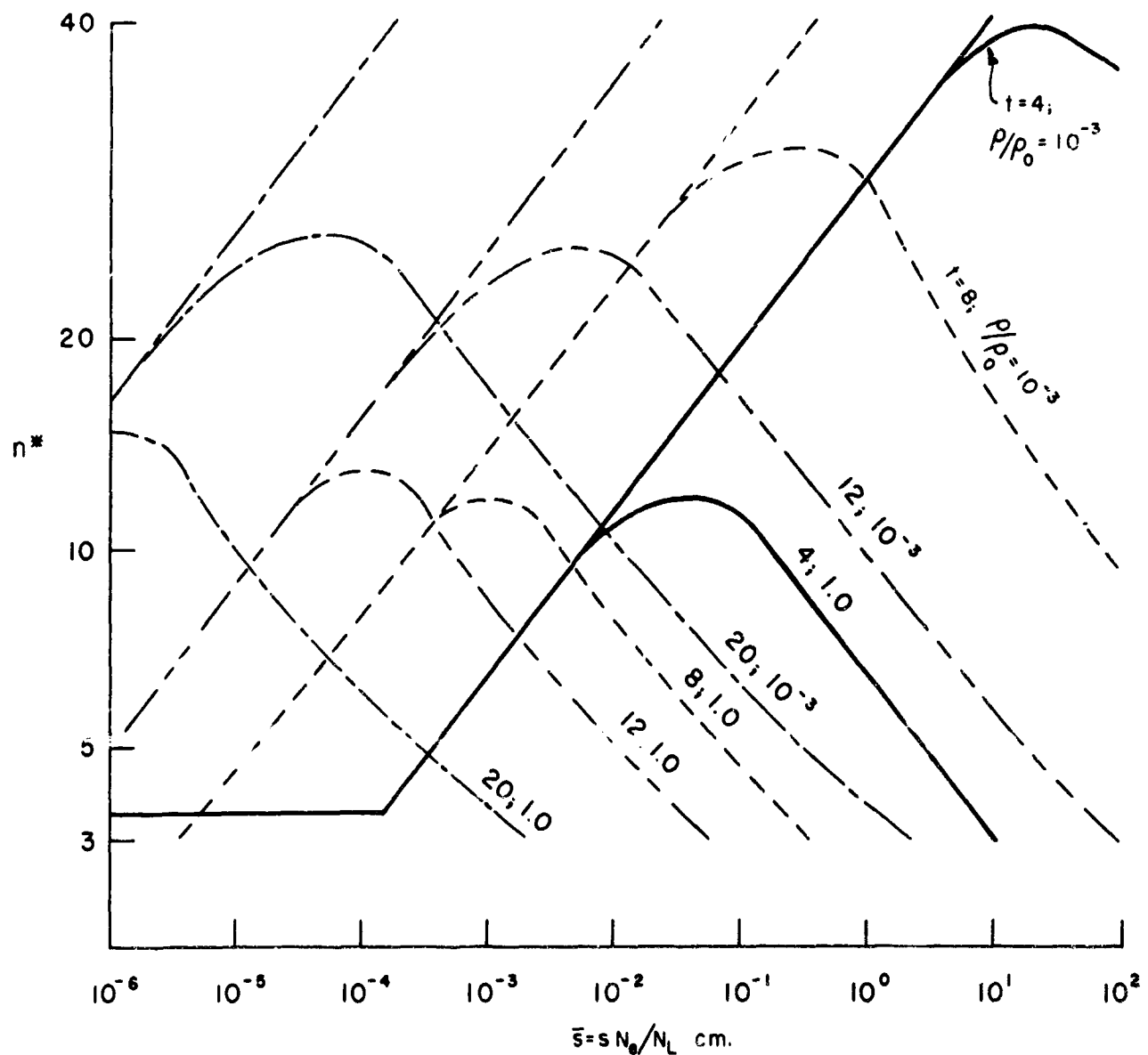
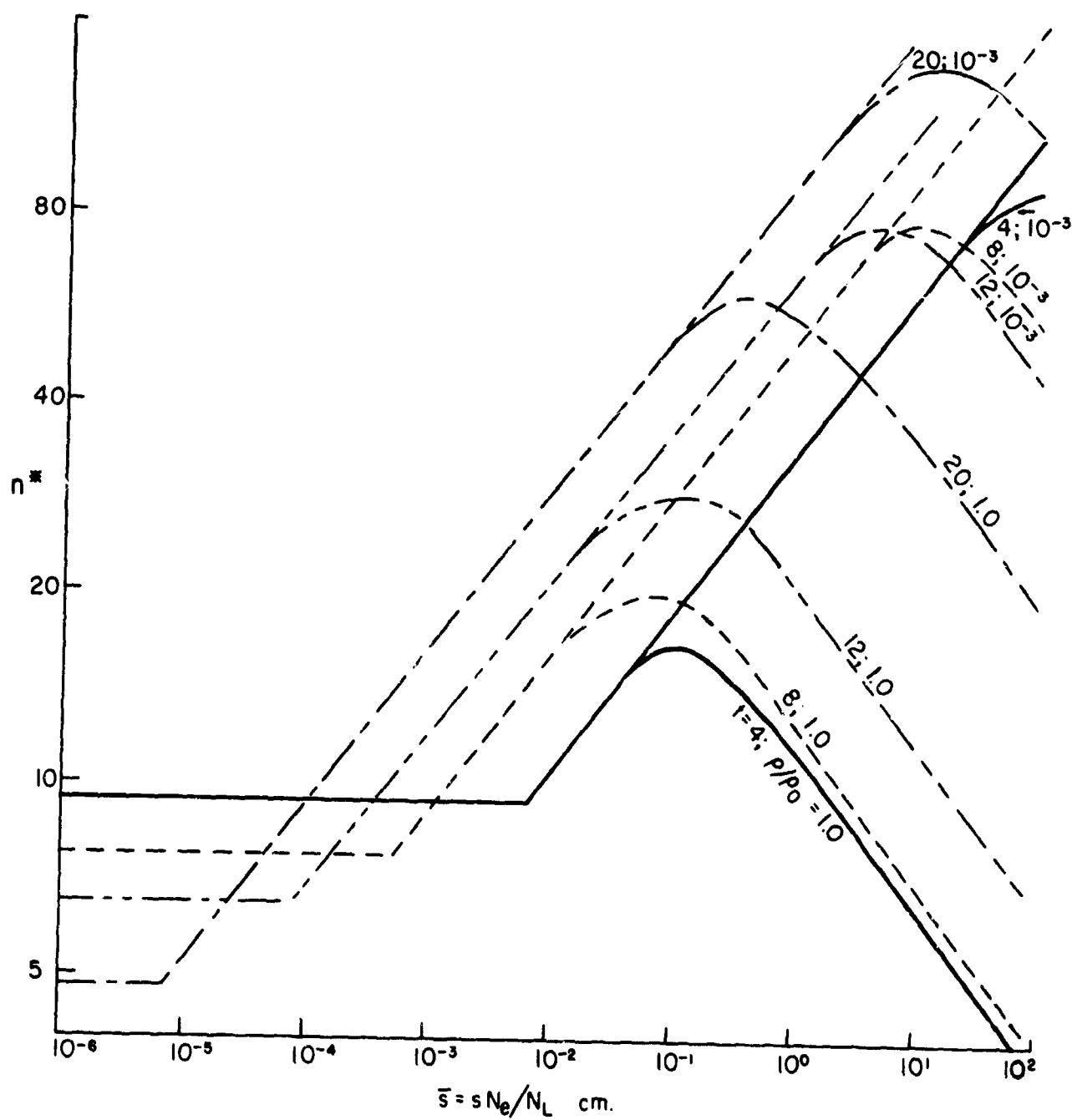
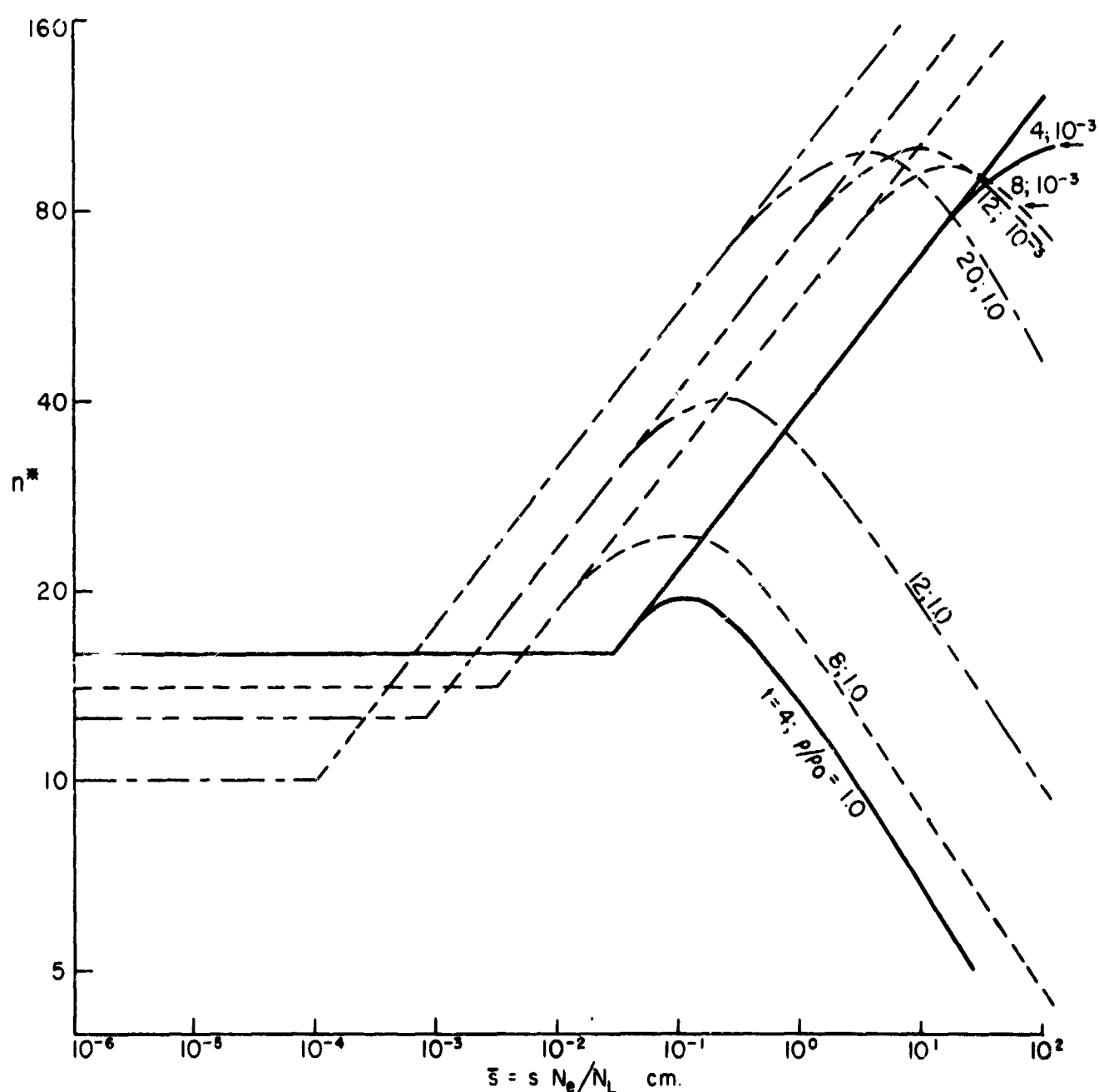


FIG. 9a VALUES OF n^* AS A FUNCTION OF ELECTRON DENSITY WEIGHTED PATH LENGTH AND INVERSE TEMPERATURE PARAMETER FOR TWO VALUES OF DENSITY.
 THE SUM OF THE INTENSITIES OF ALL LINES WITH $n \geq n^*$ IS EQUAL TO 10% OF THE INTENSITY OF THE LEADING LINE.
 $m = 1$

FIG. 9b $m = 2$

FIG. 9c $m = 3$

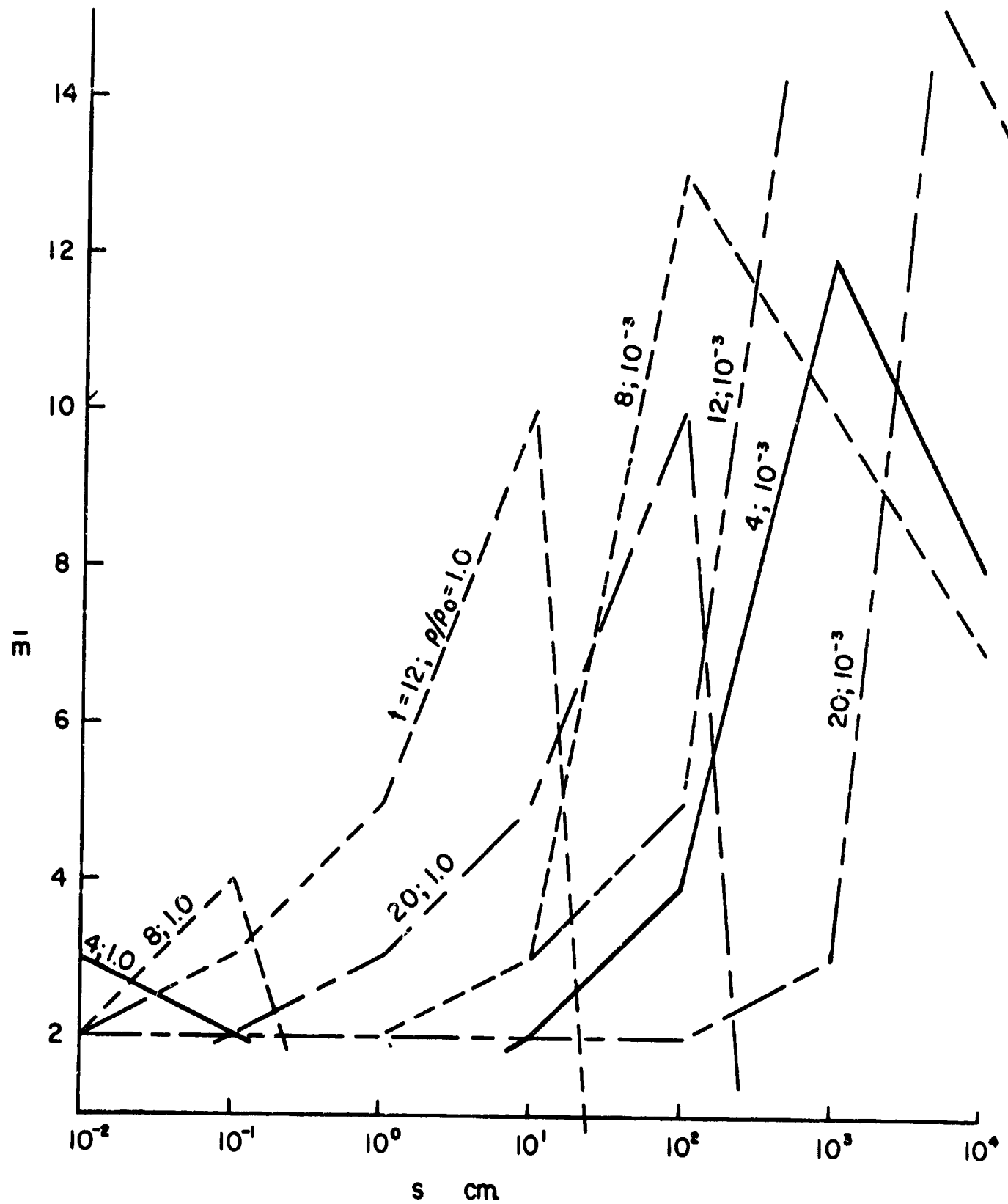


FIG. 10 LOWER STATE QUANTUM NUMBER OF FIRST COMPLETELY MERGED OR THIN SERIES.
ONLY VALUE FOR WHICH THE PATH LENGTH IS AN INTEGER POWER OF 10 HAVE MEANING.

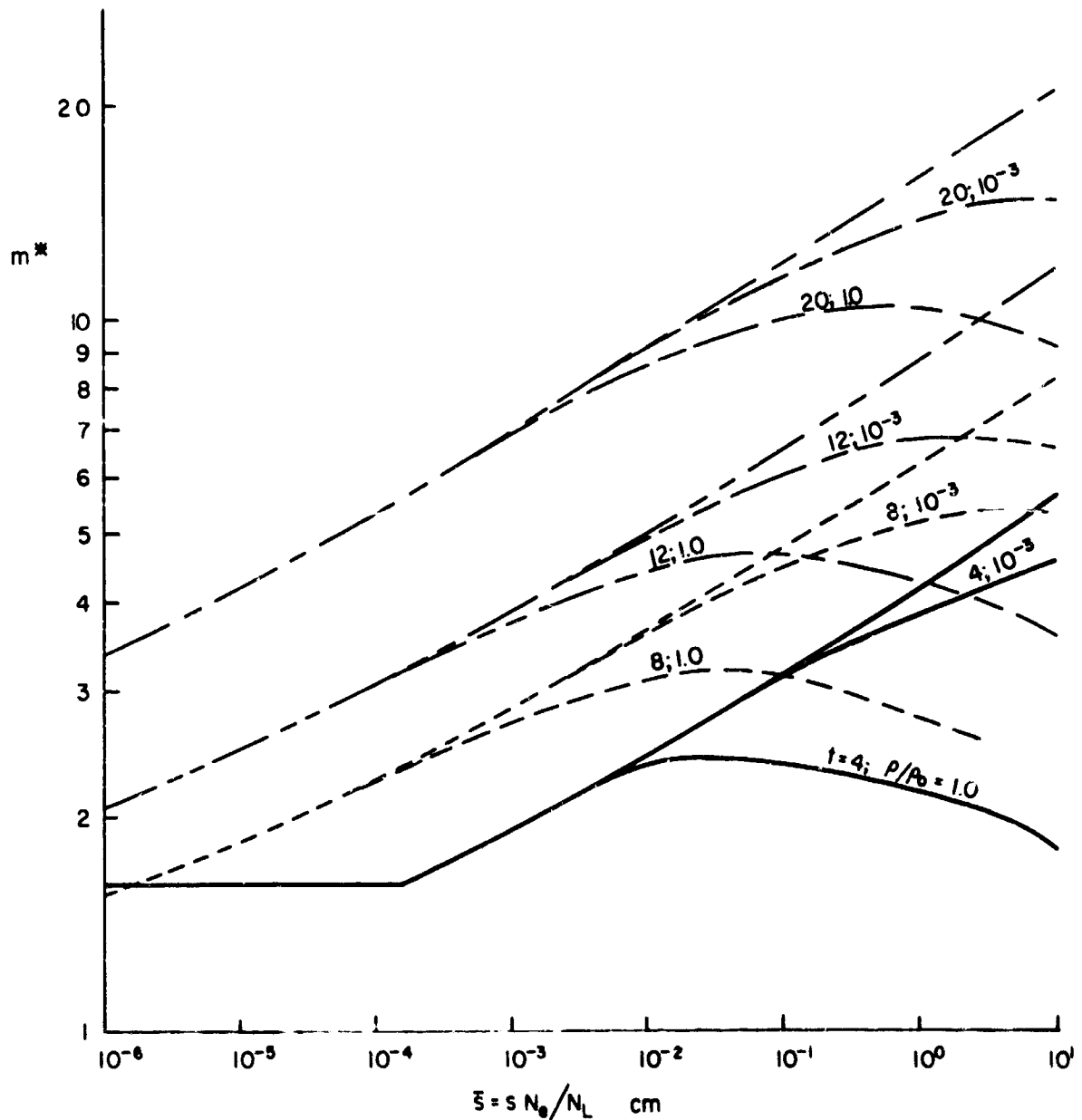


FIG. 11 VALUES OF m^* FOR HIGH SERIES AS A FUNCTION OF ELECTRON DENSITY WEIGHTED PATH LENGTH AND INVERSE TEMPERATURE PARAMETER FOR TWO VALUES OF DENSITY
 THE SUM OF THE INTENSITIES OF ALL LINES WITH $m \geq m^*$ IS EQUAL TO 10% OF THE INTENSITY OF THE RESONANCE LINE.

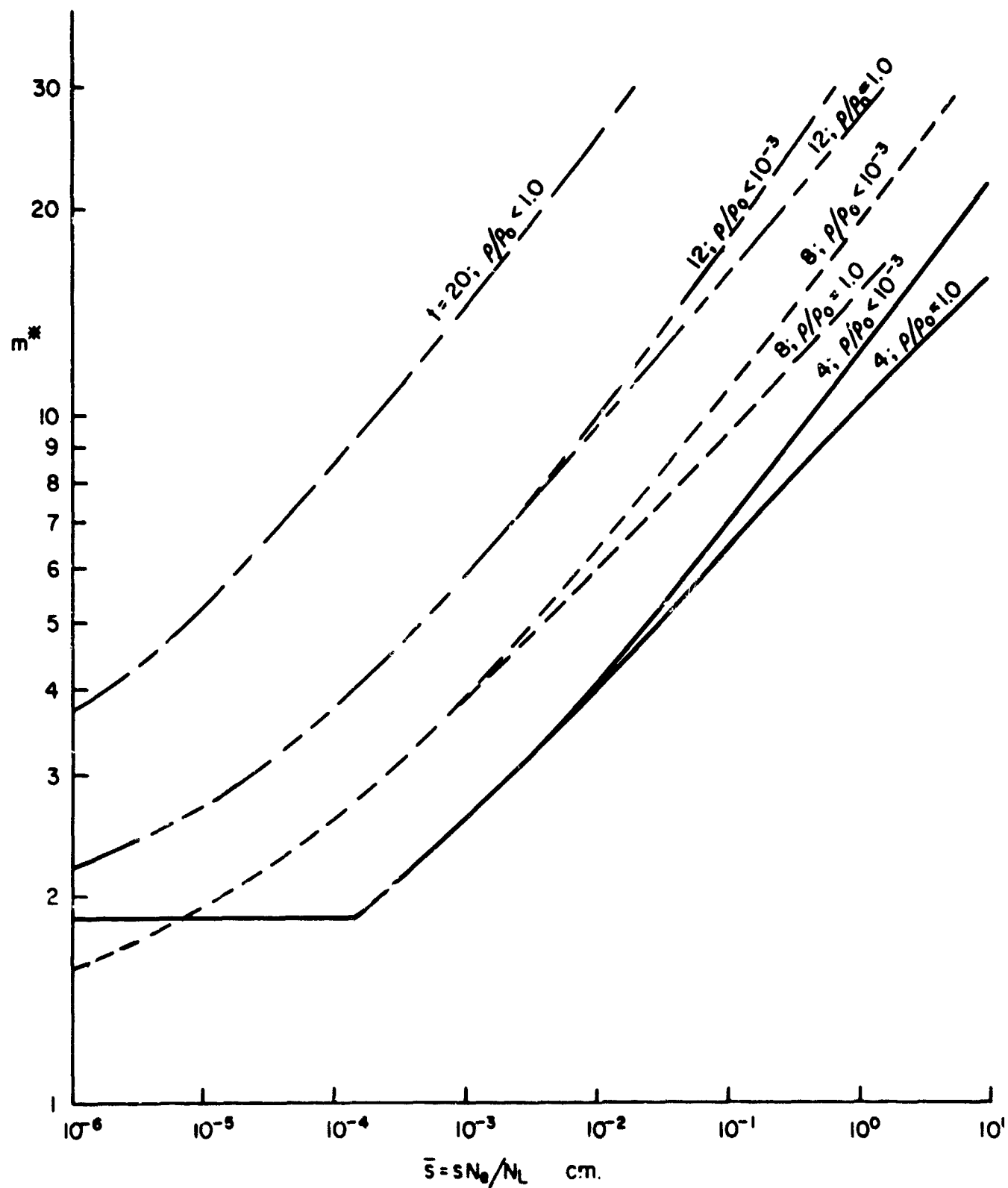


FIG. 12 VALUES OF m^* FOR HIGH SERIES PLUS HIGH PHOTOIONIZATION AS A FUNCTION OF ELECTRON DENSITY WEIGHTED PATH LENGTH AND INVERSE TEMPERATURE PARAMETER FOR TWO VALUES OF DENSITY.
 THE SUM OF THE INTENSITIES OF ALL TRANSITIONS WITH $m \geq m^*$ IS EQUAL TO 10% OF THE INTENSITY OF THE RESONANCE LINE.

Unclassified

Security Classification

DOCUMENT CONTROL DATA - R&D

(Security classification of title, body of abstract and indexing annotation must be entered when the overall report is classified)

1. ORIGINATING ACTIVITY (Corporate author)		2a. REPORT SECURITY CLASSIFICATION Unclassified
Brown University, Providence, R. I. 02912		2b. GROUP
3. REPORT TITLE RADIATIVE TRANSFER IN A GAS OF UNIFORM PROPERTIES IN LOCAL THERMODYNAMIC EQUILIBRIUM PART 2: RELATIVE LINE INTENSITIES AND THE TREATMENT OF WEAK LINES		
4. DESCRIPTIVE NOTES (Type of report and inclusive dates)		
5. AUTHOR(S) (Last name, first name, initial) Hunt, Brian L. and Sibulkin, Merwin		
6. REPORT DATE December, 1966	7a. TOTAL NO. OF PAGES 56	7b. NO. OF REFS 14
8a. CONTRACT OR GRANT NO. Nonr 562(35)	9a. ORIGINATOR'S REPORT NUMBER(S) Nonr 562(35)/17	
8b. PROJECT NO. Task NR 061-132	9b. OTHER REPORT NO(S) (Any other numbers that may be assigned this report)	
9c. d. ARPA Project Code Number 2740		
10. AVAILABILITY/LIMITATION NOTICES		
11. SUPPLEMENTARY NOTES		12. SPONSORING MILITARY ACTIVITY Advanced Research Projects Agency and Office of Naval Research
13. ABSTRACT This report is concerned with the transfer of radiative energy by the lines of a gas of uniform properties in local thermodynamic equilibrium. By means of comparatively simple calculations, the relative intensities of the potentially strong lines of a simple (hydrogenic) spectrum are computed and these results are interpreted in detail. An important conclusion from these calculations is that the influences of lower state occupation number and line oscillator strength can, under some conditions, be outweighed by factors such as the line width and the local value of the Planck function. The remainder of the report is concerned with the numerous weak lines associated with high quantum numbers. It is shown that these lines can be allowed for by extending the cross sections of the appropriate continuum processes. These techniques are then used to compare the intensities of groups of weak lines with the intensities of certain strong lines.		

DD FORM 1 JAN 64 1473

Unclassified
Security Classification

Security Classification

14 KEY WORDS	LINK A		LINK B		LINK C	
	ROLE	WT	ROLE	WT	ROLE	WT
Line merging						
Radiative transfer						
Spectral lines						

INSTRUCTIONS

1. ORIGINATING ACTIVITY: Enter the name and address of the contractor, subcontractor, grantees, Department of Defense activity or other organization (corporate author) issuing the report.

2a. REPORT SECURITY CLASSIFICATION: Enter the overall security classification of the report. Indicate whether "Restricted Data" is included. Marking is to be in accordance with appropriate security regulations.

2b. GROUP: Automatic downgrading is specified in DoD Directive 5200.10 and Armed Forces Industrial Manual. Enter the group number. Also, when applicable, show that optional markings have been used for Group 3 and Group 4 as authorized.

3. REPORT TITLE: Enter the complete report title in all capital letters. Titles in all cases should be unclassified. If a meaningful title cannot be selected without classification, show title classification in all capitals in parenthesis immediately following the title.

4. DESCRIPTIVE NOTES: If appropriate, enter the type of report, e.g., interim, progress, summary, annual, or final. Give the inclusive dates when a specific reporting period is covered.

5. AUTHOR(S): Enter the name(s) of author(s) as shown on or in the report. Enter last name, first name, middle initial. If military, show rank and branch of service. The name of the principal author is an absolute minimum requirement.

6. REPORT DATE: Enter the date of the report as day, month, year, or month, year. If more than one date appears on the report, use date of publication.

7a. TOTAL NUMBER OF PAGES: The total page count should follow normal pagination procedures, i.e., enter the number of pages containing information.

7b. NUMBER OF REFERENCES: Enter the total number of references cited in the report.

8a. CONTRACT OR GRANT NUMBER: If appropriate, enter the applicable number of the contract or grant under which the report was written.

8b, 8c, & 8d. PROJECT NUMBER: Enter the appropriate military department identification, such as project number, subproject number, system numbers, task number, etc.

9a. ORIGINATOR'S REPORT NUMBER(S): Enter the official report number by which the document will be identified and controlled by the originating activity. This number must be unique to this report.

9b. OTHER REPORT NUMBER(S): If the report has been assigned any other report numbers (either by the originator or by the sponsor), also enter this number(s).

10. AVAILABILITY/LIMITATION NOTICES: Enter any limitations on further dissemination of the report, other than those

imposed by security classification, using standard statements such as:

- (1) "Qualified requesters may obtain copies of this report from DDC."
- (2) "Foreign announcement and dissemination of this report by DDC is not authorized."
- (3) "U. S. Government agencies may obtain copies of this report directly from DDC. Other qualified DDC users shall request through ."
- (4) "U. S. military agencies may obtain copies of this report directly from DDC. Other qualified users shall request through ."
- (5) "All distribution of this report is controlled. Qualified DDC users shall request through ."

If the report has been furnished to the Office of Technical Services, Department of Commerce, for sale to the public, indicate this fact and enter the price, if known.

11. SUPPLEMENTARY NOTES: Use for additional explanatory notes.

12. SPONSORING MILITARY ACTIVITY: Enter the name of the department, project office or laboratory sponsoring (paying for) the research and development. Include address.

13. ABSTRACT: Enter an abstract giving a brief and factual summary of the document indicative of the report, even though it may also appear elsewhere in the body of the technical report. If additional space is required, a continuation sheet shall be attached.

It is highly desirable that the abstract of classified reports be unclassified. Each paragraph of the abstract shall end with an indication of the military security classification of the information in the paragraph, represented as (TS), (S), (C), or (U).

There is no limitation on the length of the abstract. However, the suggested length is from 150 to 225 words.

14. KEY WORDS: Key words are technically meaningful terms or short phrases that characterize a report and may be used as index entries for cataloging the report. Key words must be selected so that no security classification is required. Identifiers, such as equipment model designation, trade name, military project code name, geographic location, may be used as key words but will be followed by an indication of technical context. The assignment of links, rules, and weights is optional.

Unclassified

Security Classification